


## Model simulation of seasonal growth of *Fucus vesiculosus* in its benthic community

Angelika Graiff <sup>1,\*</sup>, Ulf Karsten,<sup>1</sup> Hagen Radtke,<sup>3</sup> Martin Wahl <sup>2</sup>, Anja Eggert<sup>3</sup>

<sup>1</sup>Institute of Biological Sciences, Applied Ecology and Phycology, University of Rostock, Rostock, Germany

<sup>2</sup>GEOMAR Helmholtz Centre for Ocean Research Kiel, Kiel, Germany

<sup>3</sup>Department of Physical Oceanography and Instrumentation, Leibniz Institute for Baltic Sea Research Warnemünde (IOW), Rostock, Germany

### Abstract

Numerical models are a suitable tool to quantify impacts of predicted climate change on complex ecosystems but are rarely used to study effects on benthic macroalgal communities. *Fucus vesiculosus* L. is a habitat-forming macroalga in the Baltic Sea and alarming shifts from the perennial *Fucus* community to annual filamentous algae are reported. We developed a box model able to simulate the seasonal growth of the Baltic *Fucus*–grazer–epiphyte system. This required the implementation of two state variables for *Fucus* biomass in units of carbon (C) and nitrogen (N). Model equations describe relevant physiological and ecological processes, such as storage of C and N assimilates by *Fucus*, shading effects of epiphytes or grazing by herbivores on both *Fucus* and epiphytes, but with species-specific rates and preferences. Parametrizations of the model equations and required initial conditions were based on measured parameters and process rates in the near-natural Kiel Outdoor Benthocosm (KOB) experiments during the Biological Impacts of Ocean Acidification project. To validate the model, we compared simulation results with observations in the KOB experiment that lasted from April 2013 until March 2014 under ambient and climate-change scenarios, that is, increased atmospheric temperature and partial pressure of carbon dioxide. The model reproduced the magnitude and seasonal cycles of *Fucus* growth and other processes in the KOBs over 1 yr under different scenarios. Now having established the *Fucus* model, it will be possible to better highlight the actual threat of climate change to the *Fucus* community in the shallow nearshore waters of the Baltic Sea.

Coastal marine ecosystems are under increasing threat from global and regional environmental change with consequences for species distribution, community structure, and ecosystem functioning. These impacts are likely to degrade the ecological goods and services that coastal marine ecosystems provide (Hoegh-Guldberg and Bruno 2010; Sunday et al. 2012). It remains, however, often very difficult to truly quantify impacts of predicted climate change on complex ecosystems. Numerical models can make essential contributions to this. However, so far they are only sporadically used for coastal marine ecosystems dominated by benthic macroalgal communities.

\*Correspondence: angelika.graiff@uni-rostock.de

Additional Supporting Information may be found in the online version of this article.

This is an open access article under the terms of the Creative Commons Attribution-NonCommercial-NoDerivs License, which permits use and distribution in any medium, provided the original work is properly cited, the use is non-commercial and no modifications or adaptations are made.

Our goal was to develop a prognostic, numerical model to study climate change scenarios of the complex *Fucus*–grazer–epiphyte system in the Western Baltic Sea, where the bladder wrack *Fucus vesiculosus* L. is the habitat-forming and structurally important macroalga. Our work was motivated by the comprehensive data set measured in the near-natural Kiel Outdoor Benthocosm (KOB) experiments (e.g., Graiff et al. 2015b; Werner et al. 2016) during the Biological Impacts of Ocean Acidification (BIOACID) project. In this project, we investigated the effects of warming and acidification on Baltic *Fucus* and its associated community. The impact of global warming on the semi-enclosed brackish Baltic Sea system is particularly severe (BACC 2008; BACC II 2015). Mean sea-surface temperatures have increased in all seasons since 1985 (HELCOM 2013) and a rise of 3–6°C by the end of the century is predicted (Elken et al. 2015). Future CO<sub>2</sub>-induced acidification of the surface waters of the Baltic Sea is more difficult to predict. Müller et al. (2016) showed that the peculiarities of the Baltic CO<sub>2</sub> system and especially long-term changes in alkalinity influence the predictability of ocean acidification. However,

oceanographic models for the Baltic Proper project a long-term decrease in surface pH (Omstedt et al. 2012).

Perennial *Fucus* communities in the Baltic Sea facilitate diverse epiphytic algae, invertebrate, and vertebrate communities (Kautsky et al. 1992; Middelboe et al. 2006; Torn et al. 2006; Korpinen et al. 2007; Rönnbäck et al. 2007). Throughout the seasons, *Fucus* is exposed to highly variable environmental conditions, especially annual and seasonal fluctuations in pH (7.4–8.5) and temperature (<0 to 20/25°C). However, *Fucus* performance (metabolism, growth, reproduction) and, thus, competitiveness vary dramatically along this range of environmental fluctuation (Wahl et al. 2019). Furthermore, Torn et al. (2006) report on alarming shifts from the perennial *Fucus* community to a predominance of annual filamentous algae. The decline of *Fucus* lead to measureable changes both within the *Fucus* community as well as to cascading effects on higher trophic levels (Lauringson and Kotta 2006; Wikström and Kautsky 2007), including fisheries (Aneer et al. 1983; but see Kraufvelin and Salovius 2004). Elaborate field experiments revealed that these changes must be attributed to multifactorial drivers including temperature, eutrophication, and water turbidity (Wahl et al. 2011), where indirect effects may outweigh direct effects (Wahl et al. 2015a).

It was challenging to capture the complex *Fucus*–grazer–epiphyte system in a numerical model. We basically had to start from scratch as most ocean models simulate plankton dynamics and neglect benthic primary production. Only some of them were extended to coastal, photic systems comprising benthic models (Buzzelli et al. 1999; Cerco and Noel 2004). These models focus on either seagrasses or macroalgae-forming nuisance blooms in coastal systems, or macroalgae were not included at all (Solidoro et al. 1997; Buzzelli et al. 1999; Best et al. 2001; Martins and Marques 2002). Several process-based mathematical models of macroalgal growth dynamics have been developed and applied to general scenarios and specific case studies (Duarte and Ferreira 1997; Zaldívar et al. 2009; Brush and Nixon 2010; Ren et al. 2014; Hadley et al. 2015; Port et al. 2015). Seasonal growth and composition of the kelp *Saccharina latissima* (L.) C.E. Lane, C. Mayes, Druehl and G.W. Saunders were dynamically modeled by Broch and Slagstad (2012) for aquaculture, but without considering biotic interactions. Alexandridis et al. (2012) developed a first single-species model on growth and depth distribution of *Fucus* in its natural environment and under various environmental conditions.

The *Fucus* model presented here simulates the observed near-natural KOB experiments that lasted from April 2013 until March 2014. Parametrization of the model and required initial conditions were based on measured parameters and process rates in the KOBs and accompanied laboratory experiments. It was important to consider this 1-yr period as *Fucus* shows seasonal growth and reproduction. For instance, in late spring and summer, when light conditions for photosynthesis are optimal but nutrients are low, *Fucus* uses stored winter nitrogen for

rapid growth. It was therefore crucial to describe (1) the uptake of nutrients depending on external concentrations and (2) growth depending on internal nutrient storage, which potentially decouples assimilation and growth over time. These equations are also implemented in other marine macroalgae growth models (e.g., Fong et al. 1994; Brush and Nixon 2010). Incorporation of the internal state of the algae (e.g., nitrogen) has considerably improved these models, but carbon uptake is still not explicitly described in most of them (except: Broch and Slagstad 2012; Ren et al. 2014). Without separately describing the difference in uptakes between carbon and nutrients, the application of such models to a wide range of environmental systems would be compromised, particularly in coastal systems where environmental conditions vary widely. In this respect, the present model also represents an advance on the previously published single-species model by Alexandridis et al. (2012) on *Fucus* growth, primarily in its inclusion of the functional responses of carbon and nitrogen uptakes.

*Fucus*–grazer–epiphyte interactions were another focus of our *Fucus* model. Epibionts may harm macroalgae through competition for light and nutrients or by leading to increased drag (Wahl et al. 2011). Epibionts may also attract grazers that feed on both the host and the epibionts (Wahl and Hay 1995; Jormalainen et al. 2008). In addition, herbivory is intense in littoral environments (Cyr and Pace 1993) and cascading top-down food web effects have been considered important in the Baltic Sea littoral (Werner et al. 2016).

Here, we describe our *Fucus* model and compare the simulation results with the observations of the KOB experiments. The model was used to investigate the response of *Fucus* under different temperature and partial pressure of carbon dioxide ( $p\text{CO}_2$ ) conditions that were similar to those in the mesocosm experiments. To run simulations under the present and global-change scenarios, the model was forced with atmospheric (solar radiation,  $p\text{CO}_2$ ) and hydrographic (temperature, salinity, dissolved nutrients, total alkalinity) data of the Kiel Fjord, measured from April 2013 to March 2014. For simulating global-change scenarios, atmospheric  $p\text{CO}_2$  (1100 ppm) and temperature (+5°C relative to Kiel Fjord water) were enhanced according to treatments used in the KOB experiments during the BIOACID phase II project.

## Material and procedures

### Brief technical description of the KOBs and experimental design

The KOBs are located on an aluminum float moored to the pier of the GEOMAR Helmholtz Centre for Ocean Research in the inner Kiel Fjord (54°20'N; 10°09'E). The technical description, a diagram of the Benthocosm components and the experimental setup of the KOBs were described in detail by Wahl et al. (2015b). The KOBs have an inner dimension of 2 m × 2 m and were run in open-circuit mode, that is, flow through of natural seawater pumped from Kiel Fjord at 1 m

water depth. During the experiments simulated in this study, each KOB tank was divided into two independent subunits, each with a water volume of 1.47 m<sup>3</sup>. The flow-through rate was 1.8 m<sup>3</sup> d<sup>-1</sup>, that is, the water exchange rate was 1.23 d<sup>-1</sup>.

The impacts of different global change scenarios were studied with near-natural experiments that lasted over the course of at least one seasonal cycle. Outside GEOMAR, the single and combined impacts of elevated seawater temperature and *p*CO<sub>2</sub> on the brown alga *F. vesiculosus* together with its associated community (mesograzers and epiphytes) were studied in four successive experiments in the KOBs. In order to study the effects of expected global change on this *Fucus*–grazer–epiphyte system, we contrasted the ambient temperature of Kiel Fjord water with warmer water (+5°C relative to Fjord water) at two *p*CO<sub>2</sub> levels, ambient (ca. 400 ppm) vs. ca. 1100 ppm in the headspace above the KOB. Thus, four treatments were examined: (1) ambient temperature with ambient *p*CO<sub>2</sub> (Ambient), (2) ambient temperature with elevated *p*CO<sub>2</sub> (+CO<sub>2</sub>), (3) elevated temperature with ambient *p*CO<sub>2</sub> (+Temp), and (4) elevated temperature with elevated *p*CO<sub>2</sub> (+Temp +CO<sub>2</sub>). All treatments were superimposed on the natural fluctuations of all environmental variables. The elevated levels of

both factors were chosen according to climate change predictions for shallow coastal Baltic habitats over the next 100 years (Elken et al. 2015; Schneider et al. 2015).

## Model development and parametrizations

### Model structure

*F. vesiculosus* biomass was modeled in units of carbon and nitrogen in the flow-through system of one KOB in four successive seasonal experiments of 9–12 weeks duration over 1 yr (01 April 2013 until 31 March 2014). To simulate *Fucus* growth in the four separate experiments, *Fucus* biomass was virtually added at the beginning and completely removed after each simulation, as performed during the mesocosm experiments. Nitrogen and carbon cycling in the KOBs as well as their exchange in the flow-through system of the KOB were considered (Fig. 1).

Prime abiotic forcing parameters for the KOB system were photosynthetically active radiation (PAR), temperature, salinity, dissolved nutrients (dissolved inorganic nitrogen [DIN], dissolved inorganic carbon [DIC]), phosphate concentration (PO<sub>4</sub>, only for determination of phosphate alkalinity), total alkalinity and atmospheric CO<sub>2</sub> (Fig. 2 and data sources:

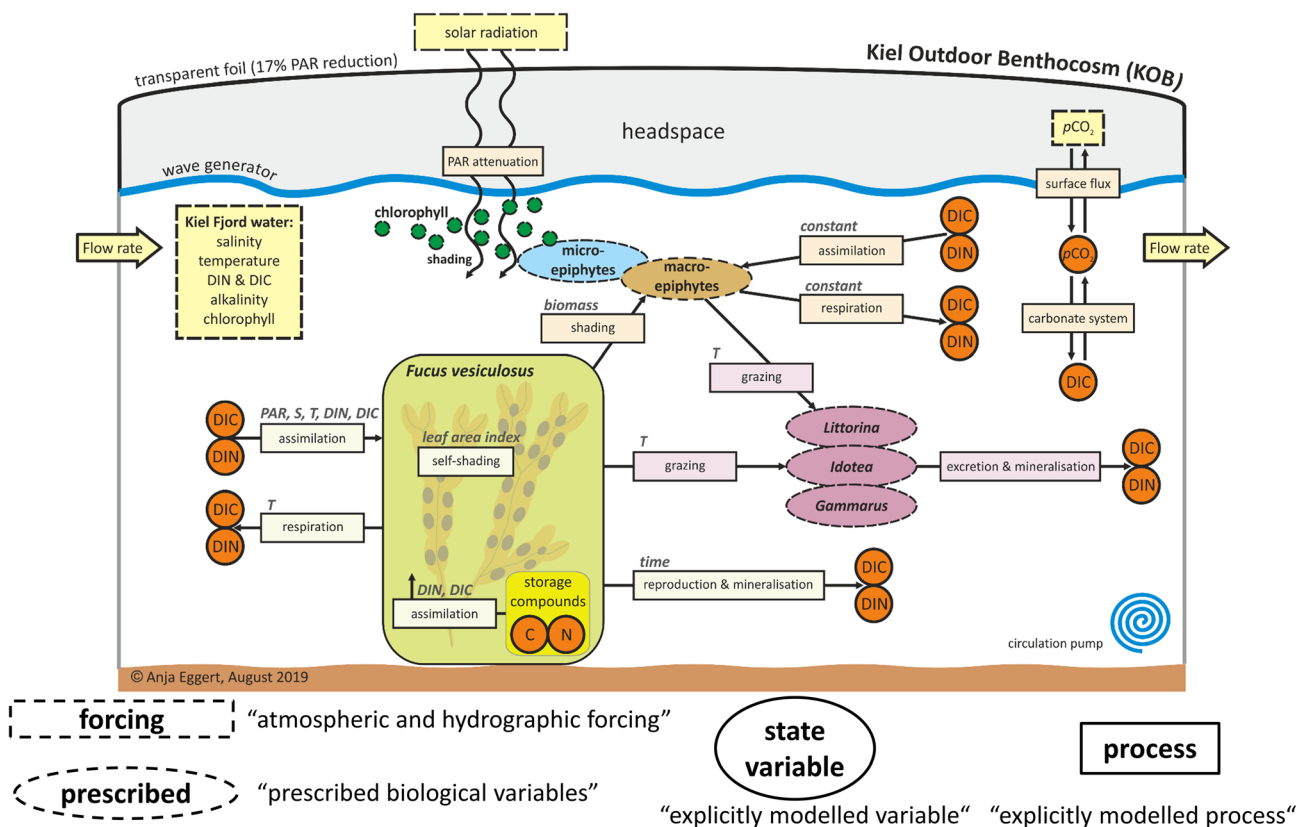


**Fig. 1.** Biogeochemical model of the *Fucus vesiculosus*–epiphyte–grazer system in a KOB. *F. vesiculosus* biomass is a state variable of the model and has a two-step uptake process where nitrogen and carbon are first stored in intracellular pools and then assimilated into the alga’s cellular structure at a rate dependent on environmental factors. Dissolved nutrients (DIN, DIC) are modeled explicitly and the nutrient exchange in the flow-through system is included. In addition, air–seawater CO<sub>2</sub> surface fluxes and the carbonate system are calculated. The implemented processes are shown in rectangles and their dependence on environmental variables is written above (PAR, temperature, salinity, dissolved nutrients).

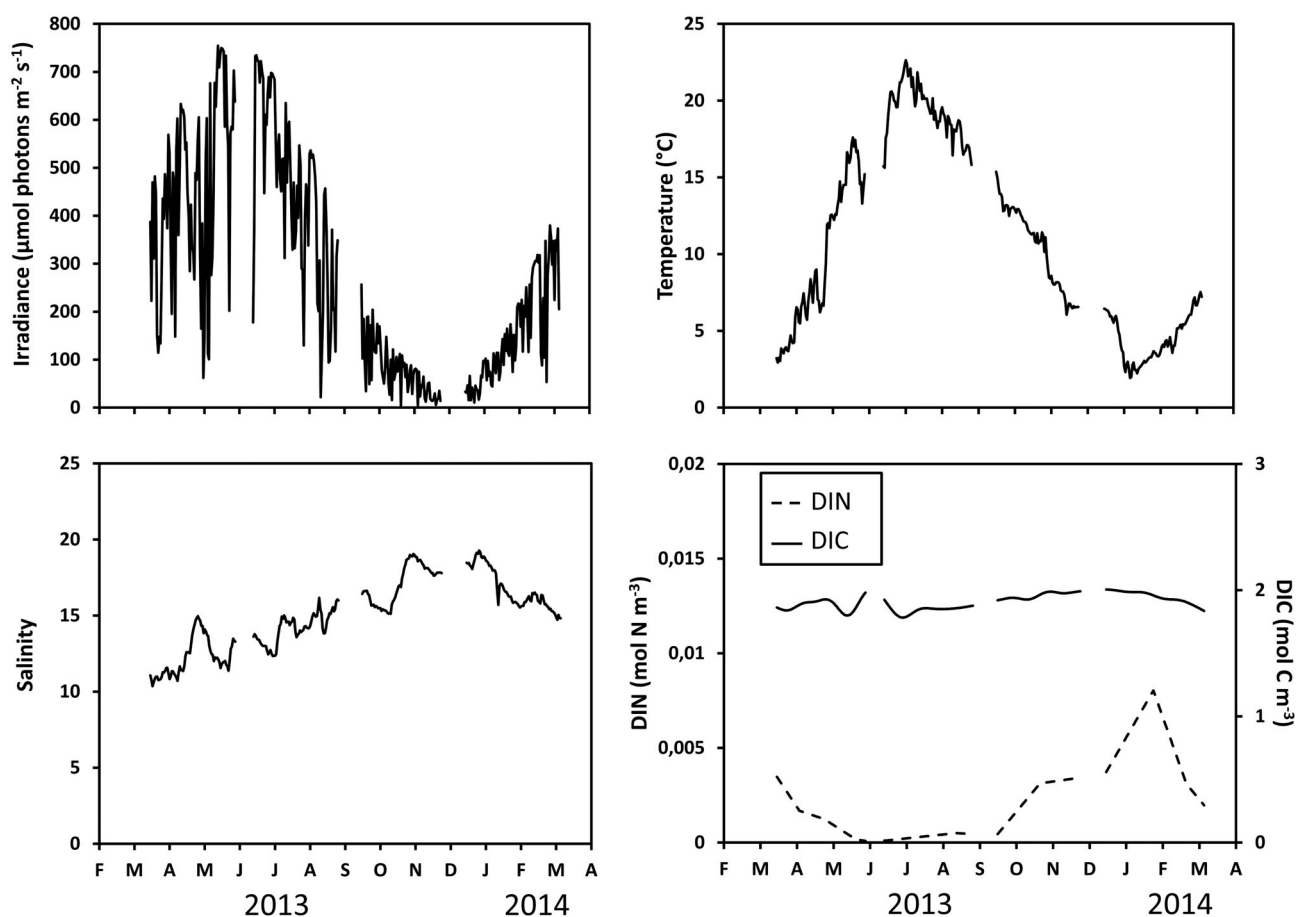


**Fig. 2.** Principal external abiotic forcing parameters for the KOB system under ambient conditions during the four successive experiments: PAR reaching the surface of the KOB, temperature in the KOB, salinity, DIN, and DIC of the Kiel Fjord water supplying the KOB in flow-through mode. The irradiance and temperature represent the range and seasonal strength in this region, with a peak in summer. Ambient DIN concentration is highest in winter. Seasons: spring: 04 April 2013–19 June 2013; summer: 04 July 2013–17 September 2013; autumn: 10 October 2013–18 December 2013; winter: 16 January 2014–01 April 2014.

Table 1). Most used data in the model were received during the BIOACID phase II project which focused on  $\text{CO}_2$  increase in the atmosphere and its influence on marine organisms. PAR data were obtained from the German Weather Service (DWD). Temperature, DIC,  $\text{PO}_4$ , total alkalinity, and atmospheric  $\text{CO}_2$  were measured during KOB experiments in the Kiel Fjord (Wahl et al. 2015b). Salinity was continuously logged in the Kiel Fjord by GEOMAR, and DIN data were obtained from the Landesamt für Landwirtschaft, Umwelt und ländliche Räume Schleswig-Holstein (LLUR).

DIC and DIN concentrations in the water were abiotic state variables with numerous source and sink terms. For example, DIN in the water of the KOBs is controlled by the amount of external DIN entering the flow-through KOB system, the rate of nitrogen assimilation by *Fucus* and photosynthetic epiphytes, and respiratory nitrogen losses by all organisms. Two biotic state variables for C and N content of *Fucus* were required because the C : N ratio varies seasonally by taking in nitrogen in excess of *Fucus* requirements when nutrients are plentiful in

winter, and by consuming internal reserves when nutrients are scarce in spring and early summer. Thus, carbon and nitrogen assimilation of *Fucus* depended on DIN and DIC concentrations in the water, while the growth rate was a function of the carbon or nitrogen reserves in the algal tissue. The dynamics of *Fucus* biomass represents the balance between nutrient assimilation, nutrient storage, respiration, grazing, and reproduction.

In order to study complex community-level effects, we first had to quantify and incorporate the (“preinteractive”) direct effects of abiotic and biotic impacts. For instance, we conducted laboratory experiments to evaluate the effect of, for example, salinity and temperature on *Fucus* growth (Bläsner and Graiff unpubl. data; Graiff et al. 2015a), shading by epiphytes (Werner et al. 2016; Wahl unpubl. data) and temperature on grazing rates of the different herbivores (Gülzow 2015; Hamer and Wahl unpubl. data). We also incorporated available data on direct effects of abiotic and biotic parameters on Baltic *Fucus*, epiphytes, and grazers derived from our own laboratory experiments or from the literature.

**Table 1.** Model input: Parameters of seasonally varying external variables.

Symbol	Description	Units	Source
$T$	Water temperature	°C	Bioacid II data
$S$	Salinity		GEOMAR—Inner Kiel Fjord
$DIN_{ext}$	Dissolved inorganic nitrogen concentration in Kiel Fjord	$mol\ m^{-3}$	LLUR—Inner Kiel Fjord
$DIC_{ext}$	Dissolved inorganic carbon concentration in Kiel Fjord	$mol\ m^{-3}$	Bioacid II data
$A_{T_{ext}}$	Total alkalinity in Kiel Fjord	$mol\ m^{-3}$	Bioacid II data
$PO4_{ext}$	Phosphate concentration in Kiel Fjord	$mol\ m^{-3}$	Bioacid II data
$PAR_{surf}$	Incident irradiance at the bottom of the KOB	$mol\ photons\ m^{-2}\ d^{-1}$	DWD—Inner Kiel Fjord
Chl	Chlorophyll $a$ concentration in Kiel Fjord water pumped through the KOB	$mg\ m^{-3}$	LLUR—Inner Kiel Fjord
$d_{microepi}$	Microepiphyte dry biomass density on <i>Fucus</i>	$mg\ cm^{-2}$	Bioacid II data
$d_{macroepi}$	Macroepiphyte dry biomass density on <i>Fucus</i>	$mg\ cm^{-2}$	Bioacid II data
RA	Reproductive allocation	$d^{-1}$	Bioacid II data
$d_I$	<i>Idotea</i> abundance in the KOB	$ind.\ m^{-3}$	Bioacid II data
$d_G$	<i>Gammarus</i> abundance in the KOB	$ind.\ m^{-3}$	Bioacid II data
$d_L$	<i>Littorina</i> abundance in the KOB	$ind.\ m^{-3}$	Bioacid II data
Sources (grazers, epis)	Decrease in carbon and nitrogen in grazers and epiphytes acted as nutrient sources for the system	$mol\ m^{-3}\ d^{-1}$	Bioacid II data
Sinks (grazers, epis)	Increase in carbon and nitrogen in grazers and epiphytes acted as nutrient sinks for the system	$mol\ m^{-3}\ d^{-1}$	Bioacid II data

Microepiphytes (mainly diatoms) and macroepiphytes (filamentous algae) were considered as prescribed biological variables, and their biomass was taken from time series measured during KOB experiments (Werner et al. 2016). Their increase or decrease in carbon and nitrogen acted as nutrient sinks or sources for the system. Thus, both groups are not explicitly modeled. However, the shading effect of microepiphyte and macroepiphyte on *Fucus* was included (Brush and Nixon 2002, Wahl unpubl. data).

Three main mesograzer taxa (*Idotea* sp., *Gammarus* sp., *Littorina* sp.) graze on both *Fucus* and macroepiphytes but with specific rates (Goecker and Kåll 2003; Gutow et al. 2016) and preferences (Goecker and Kåll 2003). They were also included as prescribed biological variables, and their biomass was taken from time series measured during KOB experiments (Werner et al. 2016). The increases or decreases in carbon and nitrogen of the grazers were included as nutrient sinks or sources for the system.

### General model equations

We developed an “open”-box model as we simulated the KOBs that run in open-circuit mode, that is, flow through of natural seawater pumped from Kiel Fjord. Accordingly, the concentration of each explicitly modeled state variable ( $T$ ) changes over time due to production ( $Q$ ) and consumption ( $S$ ) and the exchange of internal and external concentrations. The general model equation, following the Eulerian approach, can be written as

$$\frac{\partial}{\partial t} T_i = Q_i - S_i + (T_{i_{ext}} - T_i) \cdot r \quad (1)$$

where  $Q_i$  is the production and  $S_i$  is the consumption of the different state variables  $T_i$  of the *Fucus* model. In addition,  $T_i$  is determined by external ( $T_{i_{ext}}$ ) concentrations and the exchange rate  $r$ .

In such a process-oriented approach, it is assumed that several biological processes are active at the same time and contribute to  $Q_i$  and  $S_i$ . The process  $k$  is described by a turnover rate  $p_k \geq 0$ , which describes the reaction velocity of this process. Then the source and sink terms in Eq. 1 can be written as a sum over the production and consumption of this tracer by various processes:

$$Q_i = \sum_k q_{ik} p_k \quad (2)$$

and

$$S_i = \sum_k s_{ik} p_k \quad (3)$$

### Carbonate system

This study focuses on  $CO_2$  increase in the atmosphere, here in the headspace above the KOB. Therefore, the carbonate system is implemented in the model. The main variables are DIC and total alkalinity, and other derived components, for example, pH, are calculated from these. To simulate air-seawater  $CO_2$  surface fluxes, the model computes the  $pCO_2$  of the KOB water from these two variables and the phosphate concentration,

which determines the phosphate alkalinity. From the difference between atmospheric and surface-water  $p\text{CO}_2$ , the  $\text{CO}_2$  surface fluxes were parameterized as follows:

$$\text{Flux}_{\text{CO}_2} = k \cdot k_0 \cdot \Delta p\text{CO}_2 \cdot \rho_{\text{wat}}, \quad (4)$$

where  $k$  is the transfer velocity ( $\text{m d}^{-1}$ ),  $k_0$  is the solubility of  $\text{CO}_2$  ( $\text{mol kg}^{-1} \text{Pa}^{-1}$ ),  $\Delta p\text{CO}_2$  is the difference between the  $p\text{CO}_2$  in the KOB water and the air under the hood of the KOB ( $p\text{CO}_2^{\text{atm}}$ ) in Pascal (Pa), and  $\rho_{\text{wat}}$  is the water density ( $\text{kg m}^{-3}$ ). The  $\text{CO}_2$  solubility constant,  $k_0$ , depends on the temperature and salinity and was obtained from the parameterization by Weiss (1974). Symbols and units are defined in Table 2. To calculate  $p\text{CO}_2$  at the sea surface, the value-iteration method based on the equations in the DOE Handbook (1994) was used. These calculations entailed the use of thermodynamic-equilibrium constants, after Dickson and Millero (1987) and Millero (2010).

Thus, the  $\text{CO}_2$ -transfer velocity ( $k$ ) at the surface was calculated as follows:

$$k = k_{660} \cdot \left( \frac{660}{\text{Sc}(T)} \right)^{0.5}. \quad (5)$$

The Schmidt number (Sc) is defined as the ratio between the kinematic viscosity and the diffusion coefficient, which is a function of the temperature and salinity. This heuristic parametrization is based on empirical data (for details, see Schneider and Müller 2018). The exponent 0.5 is not a physical constant, but a widely used experimental approximation (Schneider and Müller 2018).

For the  $\text{CO}_2$  flux calculation, a quadratic equation for  $k_{660}$  is used, as suggested by Wanninkhof et al. (2009):

$$k_{660} = 0.24 \text{ cm h}^{-1} \cdot \left( \frac{u^2}{1 \frac{\text{m}^2}{\text{s}^2}} \right) = 0.0576 \text{ m d}^{-1} \cdot \left( \frac{u^2}{1 \frac{\text{m}^2}{\text{s}^2}} \right). \quad (6)$$

The coefficient of 0.24 applies to wind speed in  $\text{m s}^{-1}$  ( $u$ ) and gives  $k_{660}$  in  $\text{cm h}^{-1}$  or the wind speed coefficient 0.24 is multiplied by  $\frac{24}{100}$  resulting in  $\text{m d}^{-1}$ .

Import as well as export of dissolved nutrients (DIN, DIC), phosphate ( $\text{PO}_4$ ), and total alkalinity due to the flow through of natural seawater pumped from the Kiel Fjord at 1 m water depth were included as follows, for example, for DIN:

$$\text{DIN}_{\text{import}} = \text{DIN}_{\text{ext}} \cdot \left( \frac{\text{fr}}{V_{\text{box}}} \right) \quad (7)$$

and

$$\text{DIN}_{\text{export}} = \text{DIN}_{\text{int}} \cdot \left( \frac{\text{fr}}{V_{\text{box}}} \right), \quad (8)$$

where  $\text{DIN}_{\text{ext}}$  is the external DIN concentration measured in the Kiel Fjord ( $\text{mol m}^{-3}$ ) and fr is the flow rate of the water

pumped through the KOB ( $\text{m}^3 \text{d}^{-1}$ ) with a defined box volume ( $V_{\text{box}}$  in  $\text{m}^3$ ).  $\text{DIN}_{\text{int}}$  represents the internal DIN concentration in the KOB. The same procedure was used for DIC,  $A_T$  and  $\text{PO}_4$ .

### Photosynthetically active radiation

For the days from April 2013 to April 2014, downward shortwave radiation (wavelength range: 100–1000 nm, measured every 3 h) was obtained from the DWD for the location of the KOBs in the Inner Kiel Fjord. Downward shortwave radiation data in  $\text{W m}^{-2}$  were converted to  $\text{PAR}_{\text{surf}}$  (wavelength range: 400–700 nm) by applying a globally measured mean ratio of PAR to global solar radiation of 0.5 (Jacovides et al. 2003) and by converting  $1 \text{ W m}^{-2}$  of PAR to  $4.57 \mu\text{mol photons m}^{-2} \text{ s}^{-1}$  (Morel and Smith 1974). To quantify PAR attenuation in the water, we included chlorophyll concentration in addition to a background attenuation of clear water to derive the diffusive vertical attenuation coefficient ( $k_{\text{PAR}}$  in  $\text{m}^{-1}$ ):

$$k_{\text{PAR}} = k_w + k_c \cdot [\text{Chl}], \quad (9)$$

where  $k_w$  is the constant background attenuation of PAR including the effects of clear water ( $\text{m}^{-1}$ );  $k_c$  is the specific attenuation due to chlorophyll-like pigments ( $\text{m}^2 \text{mg}^{-1} \text{Chl}$ ) according to Neumann et al. (2015); and  $[\text{Chl}]$  is the chlorophyll  $a$  concentration ( $\text{mg m}^{-3}$ ), which varies seasonally. Light attenuation due to dissolved organic matter, suspended matter and detritus was neglected in our case, due to missing data.

Finally, PAR reaching the bottom of the KOB, including an additional reduction of  $\text{PAR}_{\text{surf}}$  ( $\text{mol photons m}^{-2} \text{d}^{-1}$ ) caused by the technical structure of the KOB, is calculated as follows:

$$\text{PAR}_{\text{KOB}} = \text{PAR}_{\text{surf}} \cdot e^{(-k_{\text{PAR}} \cdot z)} \cdot (1 - R_{\text{foil}}) \cdot (1 - R_{\text{KOB}}), \quad (10)$$

where  $z$  is the water depth in the KOB (m),  $R_{\text{foil}}$  is the 17% reduction of PAR caused by the transparent foil covering the KOBs (Wahl et al. 2015b), and  $R_{\text{KOB}}$  is the 20% reduction of PAR estimated for the KOB structure and shading by walls.

### Fucus primary production

#### PAR attenuation due to epiphytes and self-shading of Fucus

The incident PAR ( $\text{mol photons m}^{-2} \text{d}^{-1}$ ) reaching *Fucus* is further reduced by shading by microepiphyte and macroepiphyte and self-shading.

$$\text{PAR}_{\text{fuc}} = \text{PAR}_{\text{KOB}} \cdot (R_{\text{microepi}} + R_{\text{macroepi}}) \cdot R_{\text{self}}. \quad (11)$$

Reduction of PAR due to macroepiphyte cover ( $R_{\text{macroepi}}$ ) as a function of macroepiphyte dry mass (DM) on *Fucus* ( $d_{\text{macroepi}}$  in  $\text{mg cm}^{-2}$ ) can be described by a negative hyperbolic function with the two parameters  $A_{\text{macroepi}}$  and  $B_{\text{macroepi}}$  (Brush and Nixon 2002):

**Table 2.** Symbols, descriptions, and units of variables and parameters used in the model.

Symbol	Description	Units
$k$	Transfer velocity for CO <sub>2</sub> surface flux	m d <sup>-1</sup>
$k_0$	Solubility of CO <sub>2</sub>	mol kg <sup>-1</sup> Pa <sup>-1</sup>
$p\text{CO}_2$	Water CO <sub>2</sub> partial pressure	Pa
$p\text{CO}_2^{\text{atm}}$	Current atmospheric CO <sub>2</sub> partial pressure	Pa
$\rho_{\text{wat}}$	Water density	kg m <sup>-3</sup>
$k_{660}$	Gas exchange transfer velocity	cm h <sup>-1</sup>
$Sc(T)$	Temperature-dependent Schmidt number	Dimensionless
$u$	Wind speed	m s <sup>-2</sup>
$\text{DIN}_{\text{import}}$	Import of DIN in water pumped from Kiel Fjord	mol m <sup>-3</sup> d <sup>-1</sup>
$\text{DIN}_{\text{ext}}$	Dissolved inorganic nitrogen concentration in Kiel Fjord	mol m <sup>-3</sup>
$\text{DIN}_{\text{export}}$	Export of DIN pumped back to Kiel Fjord	mol m <sup>-3</sup> d <sup>-1</sup>
$\text{DIN}_{\text{int}}$	DIN concentration in the KOB	mol m <sup>-3</sup>
$\text{DIC}_{\text{import}}$	Import of DIC in water pumped from Kiel Fjord	mol m <sup>-3</sup> d <sup>-1</sup>
$\text{DIC}_{\text{ext}}$	DIC concentration in Kiel Fjord	mol m <sup>-3</sup>
$\text{DIC}_{\text{export}}$	Export of DIC pumped back to Kiel Fjord	mol m <sup>-3</sup> d <sup>-1</sup>
$\text{DIC}_{\text{int}}$	DIC concentration in the KOB	mol m <sup>-3</sup>
$A_{T_{\text{import}}}$	Import of alkalinity in water pumped from Kiel Fjord	mol m <sup>-3</sup> d <sup>-1</sup>
$A_{T_{\text{ext}}}$	Total alkalinity in Kiel Fjord	mol m <sup>-3</sup>
$A_{T_{\text{export}}}$	Export of alkalinity pumped back to Kiel Fjord	mol m <sup>-3</sup> d <sup>-1</sup>
$A_{T_{\text{int}}}$	Total alkalinity in the KOB	mol m <sup>-3</sup>
$\text{PO}_4_{\text{import}}$	Import of phosphate in water pumped from Kiel Fjord	mol m <sup>-3</sup> d <sup>-1</sup>
$\text{PO}_4_{\text{ext}}$	Phosphate concentration in Kiel Fjord	mol m <sup>-3</sup>
$\text{PO}_4_{\text{export}}$	Export of phosphate pumped back to Kiel Fjord	mol m <sup>-3</sup> d <sup>-1</sup>
$\text{PO}_4_{\text{int}}$	Phosphate concentration in the KOB	mol m <sup>-3</sup>
$fr$	Flow rate of the water pumped through the KOB	m <sup>3</sup> d <sup>-1</sup>
$V_{\text{box}}$	KOB box volume	m <sup>3</sup>
$k_{\text{PAR}}$	Diffusive vertical attenuation coefficient	m <sup>-1</sup>
$k_w$	Diffusive attenuation coefficient for clear ocean waters	m <sup>-1</sup>
$k_c$	Specific attenuation due to chlorophyll-like pigments	m <sup>2</sup> mg <sup>-1</sup> Chl
Chl	Chlorophyll <i>a</i> concentration in Kiel Fjord water pumped through the KOB	mg m <sup>-3</sup>
$\text{PAR}_{\text{surf}}$	Incident irradiance at the bottom of the KOB	mol photons m <sup>-2</sup> d <sup>-1</sup>
$z$	Water depth of KOB	m
$R_{\text{foil}}$	Reduction of PAR caused by the transparent foil covering the KOB	Dimensionless
$R_{\text{KOB}}$	Reduction of PAR because of the KOB structure and shading by walls	Dimensionless
$F_{\text{PAR}}$	Light limitation (PI curve)	mol photons m <sup>-2</sup> d <sup>-1</sup>
$\text{PAR}_{\text{fuc}}$	Shading-corrected PAR for <i>Fucus</i> growth	mol photons m <sup>-2</sup> d <sup>-1</sup>
$R_{\text{macroepi}}$	Attenuation of PAR as a function of macroepiphyte DM	Dimensionless
$R_{\text{microepi}}$	Attenuation of PAR as a function of microepiphyte DM	Dimensionless
$A_{\text{macroepi}}$	Parameter A of negative hyperbolic function to parameterize reduction of PAR transmission by macroepiphytes	Dimensionless
$B_{\text{macroepi}}$	Parameter B of negative hyperbolic function to parameterize reduction of PAR transmission by macroepiphytes	Dimensionless
$d_{\text{macroepi}}$	Macroepiphyte dry-biomass density on <i>Fucus</i>	mg cm <sup>-2</sup>
$A_{\text{microepi}}$	Parameter A of negative hyperbolic function to parameterize reduction of PAR transmission by microepiphytes	Dimensionless
$B_{\text{microepi}}$	Parameter B of negative hyperbolic function to parameterize reduction of PAR transmission by microepiphytes	Dimensionless
$d_{\text{microepi}}$	Microepiphyte dry-biomass density on <i>Fucus</i>	mg cm <sup>-2</sup>
LAI	Leaf area index	m <sup>2</sup> Fucus m <sup>-2</sup> KOB

(Continues)

**Table 2.** Continued

Symbol	Description	Units
$R_{\text{self}}$	self-shading of <i>Fucus</i>	Dimensionless
$G_{\text{N}}^{\text{store}}$	Gross nitrogen gain for storage	$\text{mol m}^{-3} \text{d}^{-1}$
$G_{\text{C}}^{\text{store}}$	Gross carbon gain for storage	$\text{mol m}^{-3} \text{d}^{-1}$
$\mu_{\text{N}}^{\text{store}}$	Nitrogen assimilation of <i>Fucus</i> for storage	$\text{mol m}^{-3} \text{d}^{-1}$
$Fucus_{\text{N}}^{\text{struc}}$	<i>Fucus</i> as structural nitrogen	$\text{mol N m}^{-3}$
$\mu_{\text{C}}^{\text{store}}$	Carbon assimilation of <i>Fucus</i> for storage	$\text{mol m}^{-3} \text{d}^{-1}$
$Fucus_{\text{C}}^{\text{struc}}$	<i>Fucus</i> as structural carbon	$\text{mol C m}^{-3}$
$\mu_{\text{max}}$	Maximal relative growth rate of <i>Fucus</i>	$\text{d}^{-1}$
$N_{\text{corr}}$	Factor for nitrogen uptake	Dimensionless
$C_{\text{corr}}$	Factor for carbon uptake	Dimensionless
$F_{\text{PAR}}$	PAR dependence of assimilation of <i>Fucus</i>	Dimensionless
$F_{\text{T}}$	Temperature dependence of assimilation of <i>Fucus</i>	Dimensionless
$F_{\text{S}}$	Salinity dependence of assimilation of <i>Fucus</i>	Dimensionless
$F_{\text{DIN}}$	Nitrogen limitation	Dimensionless
$F_{\text{CO}_2}$	$\text{CO}_2$ limitation	Dimensionless
$F_{\text{HCO}_3}$	$\text{HCO}_3^-$ limitation	Dimensionless
$\text{PAR}_{\text{opt}}$	PAR optimum for <i>Fucus</i> growth	$\text{mol photons m}^{-2} \text{d}^{-1}$
$T$	Temperature	$^{\circ}\text{C}$
$T_{\text{max}}$	First term coefficient of $F_{\text{T}}$ equation	$^{\circ}\text{C}$
$T_{\text{opt}}$	Second term coefficient of $F_{\text{T}}$ equation	$^{\circ}\text{C}$
$\beta_{\text{F}}$	Third term coefficient of $F_{\text{T}}$ equation	Dimensionless
$S$	Salinity	
$K_{\text{m(DIN)}}$	Half-saturation constant for DIN	$\text{mol m}^{-3}$
$\text{DIN}_{\text{int}}$	Dissolved inorganic nitrogen concentration in the KOB water	$\text{mol m}^{-3}$
$K_{\text{m(CO}_2)}$	Half-saturation constant for $\text{CO}_2$	$\text{mol kg}^{-1}$
$K_{\text{m(HCO}_3)}$	Half-saturation constant for $\text{HCO}_3^-$	$\text{mol kg}^{-1}$
$\text{CO}_2$	$\text{CO}_2$ concentration in the KOB water	$\text{mol kg}^{-1}$
$\text{HCO}_3$	$\text{HCO}_3^-$ ion concentration in the KOB water	$\text{mol kg}^{-1}$
$\mu$	<i>Fucus</i> growth dependent on carbon or nitrogen storage	$\text{mol m}^{-3} \text{d}^{-1}$
$N_{\text{reserve}}^{\text{frac}}$	Nitrogen fraction stored in <i>Fucus</i>	Dimensionless
$C_{\text{reserve}}^{\text{frac}}$	Carbon fraction stored in <i>Fucus</i>	Dimensionless
$N_{\text{min}}^{\text{struc}}$	Critical tissue concentration of nitrogen	Dimensionless
$C_{\text{min}}^{\text{struc}}$	Critical tissue concentration of carbon	Dimensionless
$Fucus_{\text{N}}^{\text{store}}$	<i>Fucus</i> as nitrogen storage	$\text{mol N m}^{-3}$
$Fucus_{\text{C}}^{\text{store}}$	<i>Fucus</i> as carbon storage	$\text{mol C m}^{-3}$
$m_{\text{N}}$	Nitrogen-specific respiration rate of <i>Fucus</i>	$\text{d}^{-1}$
$m_{\text{C}}$	Carbon-specific respiration rate of <i>Fucus</i>	$\text{d}^{-1}$
$r_0$	Relative respiration rate of <i>Fucus</i> at a reference temperature of $0^{\circ}\text{C}$	$\text{d}^{-1}$
$\beta$	Temperature coefficient	$\text{K}^{-1}$
$\text{Rep}_{\text{N}}$	Reproductive nitrogen-specific nitrogen loss in <i>Fucus</i>	$\text{mol N m}^{-3} \text{d}^{-1}$
$\text{Rep}_{\text{C}}$	Reproductive carbon-specific carbon loss in <i>Fucus</i>	$\text{mol C m}^{-3} \text{d}^{-1}$
RE	Reproductive effort	Dimensionless
RA	Reproductive allocation	$\text{d}^{-1}$
$G_{\text{I,N}}$	Nitrogen-specific grazing rate of <i>Idotea</i> on <i>Fucus</i>	$\text{mol N m}^{-3} \text{d}^{-1}$
$d_{\text{I}}$	<i>Idotea</i> abundance in the KOB	$\text{ind m}^{-3}$
$\text{GR}_{\text{I,N}}$	Maximal nitrogen-specific grazing rate of <i>Idotea</i> on <i>Fucus</i>	$\text{mol N Fucus ind}^{-1} \text{d}^{-1}$
$G_{\text{I,T}}$	Temperature factor of <i>Idotea</i> grazing	Dimensionless

(Continues)



**Table 2.** Continued

Symbol	Description	Units
FP <sub>I</sub>	Food preference of <i>Idotea</i> grazing on <i>Fucus</i>	Dimensionless
Ft <sub>N</sub>	Total food as nitrogen for grazers	mol N m <sup>-3</sup>
G <sub>I,C</sub>	Carbon-specific grazing rate of <i>Idotea</i> on <i>Fucus</i>	mol C m <sup>-3</sup> d <sup>-1</sup>
GR <sub>I,C</sub>	Maximal carbon-specific grazing rate of <i>Idotea</i> on <i>Fucus</i>	mol C <i>Fucus</i> ind <sup>-1</sup> d <sup>-1</sup>
Ft <sub>C</sub>	Total food as carbon for grazers	mol C m <sup>-3</sup>
G <sub>G,N</sub>	Nitrogen-specific grazing rate of <i>Gammarus</i> on <i>Fucus</i>	mol N m <sup>-3</sup> d <sup>-1</sup>
d <sub>G</sub>	<i>Gammarus</i> abundance in the KOB	ind m <sup>-3</sup>
GR <sub>G,N</sub>	Maximal nitrogen-specific grazing rate of <i>Gammarus</i> on <i>Fucus</i>	mol N <i>Fucus</i> ind <sup>-1</sup> d <sup>-1</sup>
G <sub>G,T</sub>	Temperature factor of <i>Gammarus</i> grazing	Dimensionless
FP <sub>G</sub>	Food preference of <i>Gammarus</i> grazing on <i>Fucus</i>	Dimensionless
G <sub>G,C</sub>	Carbon-specific grazing rate of <i>Gammarus</i> on <i>Fucus</i>	mol C m <sup>-3</sup> d <sup>-1</sup>
GR <sub>G,C</sub>	Maximal carbon-specific grazing rate of <i>Gammarus</i> on <i>Fucus</i>	mol C <i>Fucus</i> ind <sup>-1</sup> d <sup>-1</sup>
G <sub>L,N</sub>	Nitrogen-specific grazing rate of <i>Littorina</i> on <i>Fucus</i>	mol N m <sup>-3</sup> d <sup>-1</sup>
d <sub>L</sub>	<i>Littorina</i> abundance in the KOB	ind m <sup>-3</sup>
GR <sub>L,N</sub>	Maximal nitrogen-specific grazing rate of <i>Littorina</i> on <i>Fucus</i>	mol N <i>Fucus</i> ind <sup>-1</sup> d <sup>-1</sup>
G <sub>L,T</sub>	Temperature factor of <i>Littorina</i> grazing	Dimensionless
FP <sub>L</sub>	Food preference of <i>Littorina</i> grazing on <i>Fucus</i>	Dimensionless
G <sub>L,C</sub>	Carbon-specific grazing rate of <i>Gammarus</i> sp. on <i>Fucus</i>	mol m <sup>-3</sup> d <sup>-1</sup>
GR <sub>L,C</sub>	Maximal carbon-specific grazing rate of <i>Gammarus</i> sp. on <i>Fucus</i>	mol C <i>Fucus</i> ind <sup>-1</sup> d <sup>-1</sup>
T <sub>I,max</sub>	First term coefficient of G <sub>I,T</sub> equation	°C
T <sub>I,opt</sub>	Second term coefficient of G <sub>I,T</sub> equation	°C
β <sub>I</sub>	Third term coefficient of G <sub>I,T</sub> equation	Dimensionless
T <sub>G,max</sub>	First term coefficient of G <sub>G,T</sub> equation	°C
T <sub>G,opt</sub>	Second term coefficient of G <sub>G,T</sub> equation	°C
β <sub>G</sub>	Third term coefficient of G <sub>G,T</sub> equation	Dimensionless
T <sub>L,max</sub>	First term coefficient of G <sub>L,T</sub> equation	°C
T <sub>L,opt</sub>	Second term coefficient of G <sub>L,T</sub> equation	°C
β <sub>L</sub>	Third term coefficient of G <sub>L,T</sub> equation	Dimensionless

$$R_{\text{macroepi}} = 1 - A_{\text{macroepi}} \left( \frac{[d_{\text{macroepi}}]}{B_{\text{macroepi}} + [d_{\text{macroepi}}]} \right), \quad (12)$$

$$R_{\text{self}} = \min \left( 1, \frac{1}{\text{LAI}} \right). \quad (13)$$

where the applied estimates for  $A_{\text{macroepi}}$  (0.924) and  $B_{\text{macroepi}}$  (2.2) were derived by Brush and Nixon (2002).

PAR attenuation due to microepiphytes growing on the *Fucus* surface was parametrized in the same manner (Wahl unpubl. data). Macroepiphyte and microepiphyte DM was converted to biomass density on the *Fucus* surface; biomass density varies seasonally and is based on data from the KOB experiments (Werner et al. 2016). *Fucus* was clean of macroepiphytes at the beginning, and therefore their cover on *Fucus* was determined only at the end of the experiments. Microepiphyte cover was measured at the beginning and end of each experiment. Thus, we obtained time series with daily resolution, by interpolating the data for macroepiphyte and microepiphyte DM from the KOB experiments, using a simple linear relationship between the start and end of each experiment.

The PAR finally received by *Fucus* is then further reduced by self-shading.

The leaf area index (LAI) is a descriptor of the degree of leaf packing within the canopy (Watson 1947) and takes into account the leaf area that can absorb PAR. LAI values <1 describe monolayered canopies and values of LAI > 1 describe multilayered canopies. For the model, we used a mean LAI of 5.7, as determined in *Fucus* stands by Lüning (1969).

#### Carbon and nitrogen assimilation equations

Carbon and nitrogen assimilation of *Fucus* for storage ( $\mu_{\text{C}}^{\text{store}}$  [mol C m<sup>-3</sup> d<sup>-1</sup>];  $\mu_{\text{N}}^{\text{store}}$  [mol N m<sup>-3</sup> d<sup>-1</sup>]) depends on PAR, temperature, salinity, and nutrient availability. Thus, increases in gross nitrogen ( $G_{\text{N}}^{\text{store}}$  in mol N m<sup>-3</sup> d<sup>-1</sup>) and carbon ( $G_{\text{C}}^{\text{store}}$  in mol C m<sup>-3</sup> d<sup>-1</sup>) for storage are described as a function of the structural biomass  $Fucus_{\text{N}}^{\text{struc}}$  (mol N m<sup>-3</sup>) or  $Fucus_{\text{C}}^{\text{struc}}$  (mol C m<sup>-3</sup>), and maximal growth rate ( $\mu_{\text{max}}$  in d<sup>-1</sup>). The maximal growth rate,  $\mu_{\text{max}}$ , is achieved when *Fucus* is exposed to optimum light, nutrients, and temperature, assuming that no

other environmental stress is present. The value of  $\mu_{\max}$  was taken from laboratory experiments with Baltic *Fucus* grown in optimal conditions (Graiff et al. 2015a). The carbon- and nitrogen-specific gains of *Fucus* for storage are further modulated by PAR ( $F_{\text{PAR}}$ ), temperature ( $F_T$ ), and salinity dependence ( $F_S$ ) as well as by nutrient limitation ( $F_{\text{DIN}}$  or  $F_{\text{CO}_2}$ ,  $F_{\text{HCO}_3}$ ):

$$G_{\text{N}}^{\text{store}} = \mu_{\text{N}}^{\text{store}} \cdot F_{\text{N}}^{\text{struc}} = \mu_{\max} \cdot N_{\text{corr}} \cdot F_{\text{PAR}} \cdot F_T \cdot F_S \cdot F_{\text{DIN}} \cdot F_{\text{N}}^{\text{struc}} \quad (14)$$

and

$$G_{\text{C}}^{\text{store}} = \mu_{\text{C}}^{\text{store}} \cdot F_{\text{C}}^{\text{struc}} = \mu_{\max} \cdot C_{\text{corr}} \cdot F_{\text{PAR}} \cdot F_T \cdot F_S \cdot (F_{\text{CO}_2} + (1 - F_{\text{CO}_2}) \cdot 0.5 \cdot F_{\text{HCO}_3}) \cdot F_{\text{C}}^{\text{struc}}, \quad (15)$$

where  $F_T$ ,  $F_S$ ,  $F_{\text{DIN}}$ ,  $F_{\text{CO}_2}$ , and  $F_{\text{HCO}_3}$  are limitation factors that range between 0 and 1 (Supporting Information Fig. S1).

The implemented formula for the limitation factors for  $\text{CO}_2$  and bicarbonate ( $\text{HCO}_3^-$ ) take into account faster and preferred uptake of freely available  $\text{CO}_2$  under full growth rates of *Fucus*.  $\text{HCO}_3^-$  is also available in high amounts for *Fucus* in the seawater, but its uptake is energetically worse compared to free  $\text{CO}_2$  as special enzymes are required for conversion and uptake in the cells. The factors  $N_{\text{corr}}$  and  $C_{\text{corr}}$  describe the fact that assimilation into the storage pool needs to be faster under optimal nutrient conditions than the structural growth. This is required to fill up the reserves under favorable growth conditions. Since favorable DIN concentrations exist for a smaller fraction of the year, the term  $N_{\text{corr}}$  needs to exceed  $C_{\text{corr}}$ . The values 10.4 and 2.74333 were determined by model calibration, that is, by fitting the model to the actually observed sizes of the storage pools, which were measured as a relative content of nitrogen (4.3% DM) or carbon (37% DM) in *Fucus* storage (Graiff et al. 2015b).

### Limitation functions

The light-limitation function accounts for a reduction in growth caused by low irradiation and photoinhibition. The photosynthesis–irradiance (PI) relationship was described by the following equation (PI curve, Steele 1962):

$$F_{\text{PAR}} = \frac{\text{PAR}_{\text{fuc}}}{\text{PAR}_{\text{opt}}} \cdot e^{\left(1 - \frac{\text{PAR}_{\text{fuc}}}{\text{PAR}_{\text{opt}}}\right)}, \quad (16)$$

where  $\text{PAR}_{\text{fuc}}$  ( $\text{mol photons m}^{-2} \text{ d}^{-1}$ ) is the shading-corrected PAR reaching the *Fucus* surface, and  $\text{PAR}_{\text{opt}}$  ( $\text{mol photons m}^{-2} \text{ d}^{-1}$ ) is the empirical PAR optimum for *Fucus* growth (Bäck and Ruuskanen 2000).

The temperature dependence of DIC and DIN assimilation was quantified using a nonlinear regression model (Blanchard et al. 1996):

$$F_T = \left(\frac{T_{\max} - T}{T_{\max} - T_{\text{opt}}}\right)^{\beta_T} \cdot e^{\left(-\beta_T \left(\frac{T_{\max} - T}{T_{\max} - T_{\text{opt}}} - 1\right)\right)}, \quad (17)$$

with  $T \leq T_{\max}$  and  $T_{\text{opt}} < T_{\max}$ . Biomass growth was fitted against different temperature levels (5–29°C) obtained in the laboratory for *F. vesiculosus*. Growth was stopped at 26–27°C, the upper survival limit of *F. vesiculosus* in the Baltic Sea (Graiff et al. 2015a). In addition, we implemented a Heaviside step ( $\theta$ ) function to take into account lethal threshold temperatures of  $\geq 29^\circ\text{C}$  for Baltic *Fucus* (Graiff et al. 2015a).

*Fucus* biomass growth at four salinities (10, 15, 20, and 35) was obtained in the laboratory (Bläsner and Graiff unpubl. data). The highest relative growth rates were measured at a salinity of 15. Salinity dependence of N and C assimilation was based on these measured relationships. This should be viewed as a pragmatic parametrization rather than as a mechanistic description of the real process, since in reality we do not know which physiological process is affected by salinity changes and causes the differences in the relative growth rate. Linear interpolation between salinity levels yielded the relationship between biomass growth and salinity for *Fucus* ( $F_S$ ; Supporting Information).

Nitrogen uptake is described with a Michaelis–Menten equation with squared arguments according to Fennel and Neumann (1996), to smooth the dynamics of mean DIN values at smaller concentrations:

$$F_{\text{DIN}} = \frac{\text{DIN}_{\text{int}}^2}{K_{\text{m(DIN)}}^2 + \text{DIN}_{\text{int}}^2}, \quad (18)$$

where  $K_{\text{m(DIN)}}$  ( $\text{mol m}^{-3}$ ) is the half-saturation constant, or the substrate concentration supporting half of the maximum rate of DIN uptake (Wallentinus 1984), and  $\text{DIN}_{\text{int}}$  is the concentration ( $\text{mol m}^{-3}$ ) in the KOB water.

Accordingly, we described the uptake of  $\text{CO}_2$  and bicarbonate ( $\text{HCO}_3^-$ ) with a modified Michaelis–Menten equation with squared arguments (Fennel and Neumann 1996), which results in a sigmoid functional response:

$$F_{\text{CO}_2} = \frac{\text{CO}_2^2}{K_{\text{m(CO}_2)}^2 + \text{CO}_2^2} \quad (19)$$

and

$$F_{\text{HCO}_3} = \frac{\text{HCO}_3^2}{K_{\text{m(HCO}_3)}^2 + \text{HCO}_3^2}, \quad (20)$$

where  $K_{\text{m(CO}_2)}$  ( $\text{mol kg}^{-1}$ ) and  $K_{\text{m(HCO}_3)}$  ( $\text{mol kg}^{-1}$ ) are the half-saturation constants of  $\text{CO}_2$  and  $\text{HCO}_3^-$  uptake (Sand-Jensen and Gordon 1984), as well as  $\text{CO}_2$  and  $\text{HCO}_3^-$  concentrations ( $\text{mol kg}^{-1}$ ) in the KOB water. Most marine algal species acquire dissolved inorganic carbon in the form of  $\text{CO}_2$  and many species also possess carbon-concentrating mechanisms (CCMs) to satisfy their photosynthetic carbon demand (reviewed in Raven et al. 2011). CCMs enable these algae to acquire inorganic carbon from the seawater by direct uptake of  $\text{HCO}_3^-$

and/or its conversion to CO<sub>2</sub> through the action of internal and/or external carbonic anhydrase (Badger 2003; Giordano et al. 2005; Hepburn et al. 2011). An inorganic carbon-concentrating mechanism is suggested to operate in *Fucus* species (Kerby and Raven 1985; Johnston and Raven 1990). Thus, we considered uptake of both CO<sub>2</sub> and HCO<sub>3</sub><sup>-</sup> by *Fucus* (Sand-Jensen and Gordon 1984).

### Equations for internal reserves and growth rates

*Fucus* stores carbon and nitrogen compounds. Accordingly, the C/N ratio is not constant and varies seasonally (Graiff et al. 2015b). Thus, we modeled *Fucus* growth as a two-step coupled function; uptake is dependent on the external nutrient concentration, and growth ( $\mu$  in mol m<sup>-3</sup> d<sup>-1</sup>) is dependent on the internal carbon and nitrogen concentrations (see, e.g., Fong et al. 1994; Solidoro et al. 1997; Aldridge and Trimmer 2009; Port et al. 2015).

$$\mu = \mu_{\max} \cdot \min \left( \frac{N_{\text{reserve}}^{\text{frac}}}{(N_{\text{reserve}}^{\text{frac}} + N_{\text{min}}^{\text{struc}})}, \frac{C_{\text{reserve}}^{\text{frac}}}{(C_{\text{reserve}}^{\text{frac}} + C_{\text{min}}^{\text{struc}})} \right). \quad (21)$$

Thus, *Fucus* growth ( $\mu$ ) depends on the maximal growth rate ( $\mu_{\max}$ ; Graiff et al. 2015a), the nitrogen ( $N_{\text{reserve}}^{\text{frac}}$ ) and carbon ( $C_{\text{reserve}}^{\text{frac}}$ ) fractions stored in the *Fucus* tissue, and the critical tissue concentrations of nitrogen ( $N_{\text{min}}^{\text{struc}}$ ) and carbon ( $C_{\text{min}}^{\text{struc}}$ ). In our model, we used 1.7% reserve nitrogen (Pedersen and Borum 1996) and 10% carbon (Duarte 1992), respectively, as a fraction of tissue biomass and the minimum structural requirement for growth. If uptake and growth rates are similar, then internal nutrient reserves will not accumulate and growth will track the nutrient concentrations in the environment. If uptake exceeds growth, then nitrogen and/or carbon will be stored in the algal tissue.

The fraction of stored nitrogen ( $N_{\text{reserve}}^{\text{frac}}$ ) or carbon ( $C_{\text{reserve}}^{\text{frac}}$ ) in the algal tissue is defined as

$$N_{\text{reserve}}^{\text{frac}} = \frac{Fucus_{\text{N}}^{\text{store}}}{(Fucus_{\text{N}}^{\text{store}} + Fucus_{\text{N}}^{\text{struc}})} \quad (22)$$

and

$$C_{\text{reserve}}^{\text{frac}} = \frac{Fucus_{\text{C}}^{\text{store}}}{(Fucus_{\text{C}}^{\text{store}} + Fucus_{\text{C}}^{\text{struc}})}, \quad (23)$$

where  $Fucus_{\text{N}}^{\text{store}}$  (mol N m<sup>-3</sup>) and  $Fucus_{\text{C}}^{\text{store}}$  (mol C m<sup>-3</sup>) are the concentrations of stored nitrogen or carbon in the *Fucus* tissue which can be incorporated into structural components ( $Fucus_{\text{N}}^{\text{struc}}$  [mol N m<sup>-3</sup>];  $Fucus_{\text{C}}^{\text{struc}}$  [mol C m<sup>-3</sup>]) of the alga during growth. Stored and structural nitrogen or carbon depend on the initial total *Fucus* biomass in each season in the KOB (Table 3). Seasonally adjusted proportions of stored or

**Table 3.** Model input: initial *Fucus vesiculosus* biomass as carbon (C) and nitrogen (N) in each KOB experiment, as well as the seasonally adjusted proportions of carbon and nitrogen for *Fucus* structure and storage.

Season	Initial C (mol m <sup>-3</sup> )	Initial N (mol m <sup>-3</sup> )		C (%)	N (%)
Spring	0.221	0.010	Structural	75	80
			Stored	25	20
Summer	0.140	0.006	Structural	55	94
			Stored	45	6
Autumn	0.146	0.007	Structural	72	98
			Stored	28	2
Winter	0.081	0.004	Structural	90	85
			Stored	10	15

structural nitrogen and carbon were chosen according to nitrogen and carbon contents of *Fucus* measured during the KOB experiments (Graiff et al. 2015b). Thus, any excess nitrogen and carbon is stored, and the amount stored controls the rate of growth. This allows the modeled *Fucus* to take up nitrogen and carbon when available in the water, but modulated by PAR, temperature, and salinity, and to grow later when dissolved nutrient concentrations are low in the water using stored nutrients.

### Fucus loss terms

Loss terms for *Fucus* biomass include respiration, reproduction, and grazing by the most abundant herbivores in the Baltic Sea.

#### Respiration

The main factor controlling respiration of algae is temperature (Lüning 1990), and this relationship is described by the mainly empirical Q<sub>10</sub> formulation (van't Hoff 1884). This formulation is applied to both terms constituting nitrogen- and carbon-specific respiration:

$$rm_{\text{N}} = r_0 \cdot e^{(\beta \cdot T)} \cdot Fucus_{\text{N}}^{\text{struc}} \quad (24)$$

and

$$rm_{\text{C}} = r_0 \cdot e^{(\beta \cdot T)} \cdot Fucus_{\text{C}}^{\text{struc}}. \quad (25)$$

The coefficient  $\beta$  (K<sup>-1</sup>) of temperature limitation is equivalent to an increase in respiration by a factor of 2 for every 10°C increase in temperature ( $T$ ), while  $r_0$  (d<sup>-1</sup>) is the relative respiration rate of *Fucus* at a reference temperature of 0°C (Markager and Sand-Jensen 1992).

#### Reproduction

Carbon and nitrogen losses due to reproduction of *Fucus* were considered. The biomass produced by the vegetative

**Table 4.** Model input: constant parameters and references.

Parameter	Value	Units	Source
$u$	15	$\text{m s}^{-1}$	
$p\text{CO}_2^{\text{atm}}$	40.5 or 111	Pa	Bioacid II data
$fr$	1.8	$\text{m}^3 \text{d}^{-1}$	Wahl et al. (2015b)
$V_{\text{box}}$	1.47	$\text{m}^3$	Wahl et al. (2015b)
$k_w$	0.027	$\text{m}^{-1}$	Smith and Baker (1978)
$k_c$	0.029	$\text{m}^2 \text{mg}^{-1} \text{Chl}$	Neumann et al. (2015)
$z$	0.3675	m	Wahl et al. (2015b)
$R_{\text{foil}}$	0.17	Dimensionless	Wahl et al. (2015b)
$R_{\text{KOB}}$	0.2	Dimensionless	
$A_{\text{microepi}}$	1.0837	Dimensionless	Wahl et al. (unpubl. data)
$B_{\text{microepi}}$	1.3797	Dimensionless	Wahl et al. (unpubl. data)
$A_{\text{macroepi}}$	0.924	Dimensionless	Brush and Nixon (2002)
$B_{\text{macroepi}}$	2.2	Dimensionless	Brush and Nixon (2002)
LAI	5.7	$\text{m}^2 \text{Fucus m}^{-2}$	Lüning (1969)
$\text{PAR}_{\text{opt}}$	21.6	$\text{mol photons m}^{-2} \text{d}^{-1}$	Bäck and Ruuskanen (2000)
$\mu_{\text{max}}$	0.047	$\text{d}^{-1}$	Graiff et al. (2015a)
$N_{\text{corr}}$	10.4	Dimensionless	Derived from Graiff et al. (2015b)
$C_{\text{corr}}$	2.74333	Dimensionless	Derived from Graiff et al. (2015b)
$T_{\text{max}}$	33.15	$^{\circ}\text{C}$	Derived from Graiff et al. (2015a)
$T_{\text{opt}}$	16.76	$^{\circ}\text{C}$	Derived from Graiff et al. (2015a)
$\beta_{\text{F}}$	3.333	Dimensionless	Derived from Graiff et al. (2015a)
$K_{\text{m}(\text{CO}_2)}$	0.00028	$\text{mol kg}^{-1}$	Sand-Jensen and Gordon (1984)
$K_{\text{m}(\text{HCO}_3)}$	0.00054	$\text{mol kg}^{-1}$	Sand-Jensen and Gordon (1984)
$K_{\text{m}(\text{DIN})}$	0.0073	$\text{mol m}^{-3}$	Wallentinus (1984)
$N_{\text{min}}^{\text{struc}}$	0.017	Dimensionless	Pedersen and Borum (1996)
$C_{\text{min}}^{\text{struc}}$	0.1	Dimensionless	Duarte (1992)
$r_0$	0.0027	$\text{d}^{-1}$	Markager and Sand-Jensen (1992)
$\beta$	0.0693	$\text{K}^{-1}$	
RE	0.18	Dimensionless	Brenchley et al. (1996)
$\text{GR}_{\text{I,N}}$	$1.207 \times 10^{-6}$	$\text{mol N Fucus ind}^{-1} \text{d}^{-1}$	Goecker and Käll (2003)
$\text{FP}_{\text{I}}$	7.7	Dimensionless	Goecker and Käll (2003)
$\text{GR}_{\text{I,C}}$	$24.632 \times 10^{-6}$	$\text{mol C Fucus ind}^{-1} \text{d}^{-1}$	Goecker and Käll (2003)
$\text{GR}_{\text{G,N}}$	$0.176 \times 10^{-6}$	$\text{mol N Fucus ind}^{-1} \text{d}^{-1}$	Goecker and Käll (2003)
$\text{FP}_{\text{G}}$	1.2	Dimensionless	Goecker and Käll (2003)
$\text{GR}_{\text{G,C}}$	$3.592 \times 10^{-6}$	$\text{mol C Fucus ind}^{-1} \text{d}^{-1}$	Goecker and Käll (2003)
$\text{GR}_{\text{L,N}}$	$0.402 \times 10^{-6}$	$\text{mol N Fucus ind}^{-1} \text{d}^{-1}$	Gutow et al. (2016)
$\text{FP}_{\text{L}}$	1	Dimensionless	
$\text{GR}_{\text{L,C}}$	$8.891 \times 10^{-6}$	$\text{mol C Fucus ind}^{-1} \text{d}^{-1}$	Gutow et al. (2016)
$T_{\text{I,max}}$	30.469	$^{\circ}\text{C}$	Derived from Güllow (2015)
$T_{\text{I,opt}}$	23.242	$^{\circ}\text{C}$	Derived from Güllow (2015)
$\beta_{\text{I}}$	1.217	Dimensionless	Derived from Güllow (2015)
$T_{\text{G,max}}$	30.632	$^{\circ}\text{C}$	Derived from Güllow (2015)
$T_{\text{G,opt}}$	19.143	$^{\circ}\text{C}$	Derived from Güllow (2015)
$\beta_{\text{G}}$	12.179	Dimensionless	Derived from Güllow (2015)
$T_{\text{L,max}}$	27.259	$^{\circ}\text{C}$	Derived from Hamer and Wahl (unpubl. data)
$T_{\text{L,opt}}$	16.895	$^{\circ}\text{C}$	Derived from Hamer and Wahl (unpubl. data)
$\beta_{\text{L}}$	3.39	Dimensionless	Derived from Hamer and Wahl (unpubl. data)

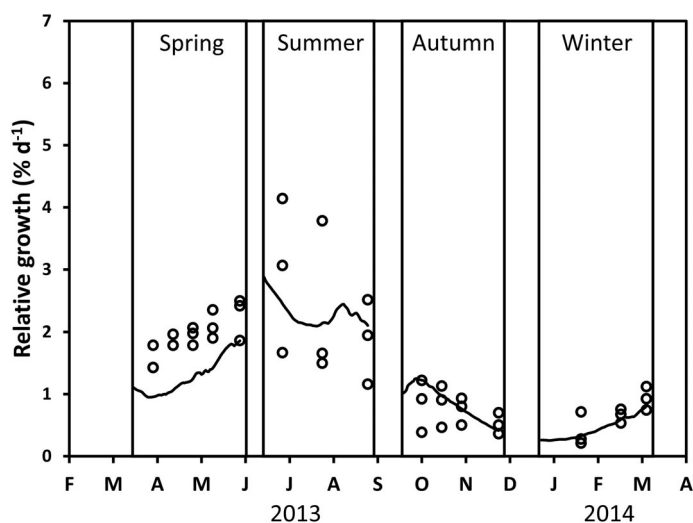


**Fig. 3.** Measured (points) and modeled (lines) relative growth rates of *Fucus vesiculosus* during experiments in the KOB, with ambient temperature and  $p\text{CO}_2$  conditions over different seasons. Seasons: spring: 04 April 2013–19 June 2013; summer: 04 July 2013–17 September 2013; autumn: 10 October 2013–18 December 2013; winter: 16 January 2014–01 April 2014. Data are from the length–growth measurements of Graiff et al. (2015b).

parts of the alga is allocated to the receptacles during their development and lost after their abscission. Development of the reproductive tissue (reproductive allocation [RA]) was calculated according to Robertson (1987) at the end of each KOB experiment. RA reflects the amount of carbon and nitrogen allocated to the reproductive tissue per unit time, relative to the carbon or nitrogen content in the plant's vegetative tissue. However, RA alone is not sufficient to assess the cost for a *Fucus* individual, because the reproductive tissue itself contributes its own photosynthetic production (Brenchley et al. 1996).

**Table 5.** RMSD measurements, absolute value of the Pbias, and coefficients of determination ( $R^2$ ) of the differences between values predicted by the model and the values actually observed for *Fucus vesiculosus* growth and pH during experiments in the KOB, with various temperature and  $p\text{CO}_2$  conditions over different seasons. Seasons: spring: 04 April 2013–19 June 2013; summer: 04 July 2013–17 September 2013; autumn: 10 October 2013–18 December 2013; winter: 16 January 2014–01 April 2014. Temperature and  $p\text{CO}_2$  conditions: Ambient: ambient temperature and  $p\text{CO}_2$ , + $\text{CO}_2$ : ambient temperature and elevated  $p\text{CO}_2$ , +Temp: elevated temperature and ambient  $p\text{CO}_2$ , +Temp + $\text{CO}_2$ : elevated temperature and  $p\text{CO}_2$ .

		Ambient			+ $\text{CO}_2$			+Temp			+Temp + $\text{CO}_2$		
		RMSD	Pbias	$R^2$	RMSD	Pbias	$R^2$	RMSD	Pbias	$R^2$	RMSD	Pbias	$R^2$
Growth	Spring	0.65	-32.66	0.86	1.38	-50.38	0.37	1.45	-45.61	0.44	1.39	-44.79	0.30
	Summer	0.33	-6.23	0.91	1.24	-31.66	0.89	0.03	2.98	1.00	0.64	-34.96	1.00
	Autumn	0.21	-14.37	0.89	0.09	-8.78	0.98	0.18	19.32	0.97	0.13	14.15	0.99
	Winter	0.09	-13.07	0.99	0.26	-28.43	0.99	0.38	43.76	0.99	0.17	1.40	0.98
pH	Spring	0.36	-2.33	0.46	0.49	-4.26	0.35	0.28	-1.17	0.41	0.35	-2.40	0.37
	Summer	0.14	-0.01	0.39	0.19	-1.75	0.35	0.19	0.88	0.51	0.19	-0.67	0.47
	Autumn	0.19	-2.19	0.13	0.30	-3.61	0.22	0.19	-2.18	>0.01	0.28	-3.49	0.11
	Winter	0.25	-2.73	0.06	0.25	-3.12	>0.01	0.19	-1.77	0.25	0.23	-2.45	0.50

The proportion of reproductive carbon and nitrogen requirements contributed by receptacle photosynthesis is termed the reproductive effort (RE; Brenchley et al. 1996). RE was measured by Brenchley et al. (1996) as the proportion of receptacle carbon cost, that is, receptacle growth plus receptacle respiration made up by receptacle photosynthesis. The reproduction-related nitrogen- and carbon-specific losses ( $\text{mol m}^{-3} \text{d}^{-1}$ ) during receptacle development were formulated as

$$\text{Rep}_N = (1 - \text{RE}) \cdot \text{RA} \cdot \text{Fucus}_N^{\text{struc}} \quad (26)$$

and

$$\text{Rep}_C = (1 - \text{RE}) \cdot \text{RA} \cdot \text{Fucus}_C^{\text{struc}}. \quad (27)$$

A continuous time series with daily resolution was obtained for RA ( $\text{d}^{-1}$ ) using linear interpolation between experiments. Carbon and nitrogen released during these loss processes were assumed to be directly mineralized and added to the pool of free available DIN and DIC in the KOB water.

#### Herbivory

Grazing rates on *Fucus* are highly variable but can be a significant loss term (e.g., Engkvist et al. 2000; Jormalainen et al. 2001; Wahl et al. 2011). The most abundant grazers in the *Fucus*-associated mesofauna are gammarid amphipods, isopods of the genus *Idotea*, and the gastropod *Littorina littorea* (L.) (Anders and Möller 1983). The preferential grazing on *Fucus* and epiphytes is regarded as an important regulatory mechanism, which can strongly affect structure and biomass accumulation in macroalgal communities (Hillebrand et al. 2000; Goecker and Käll 2003; Korpinen et al. 2007). Grazing-related nitrogen- and carbon-specific losses of *Fucus* were modeled separately for *Idotea* sp., *Gammarus* sp. and *L. littorea*, with specific rates, temperature dependences and

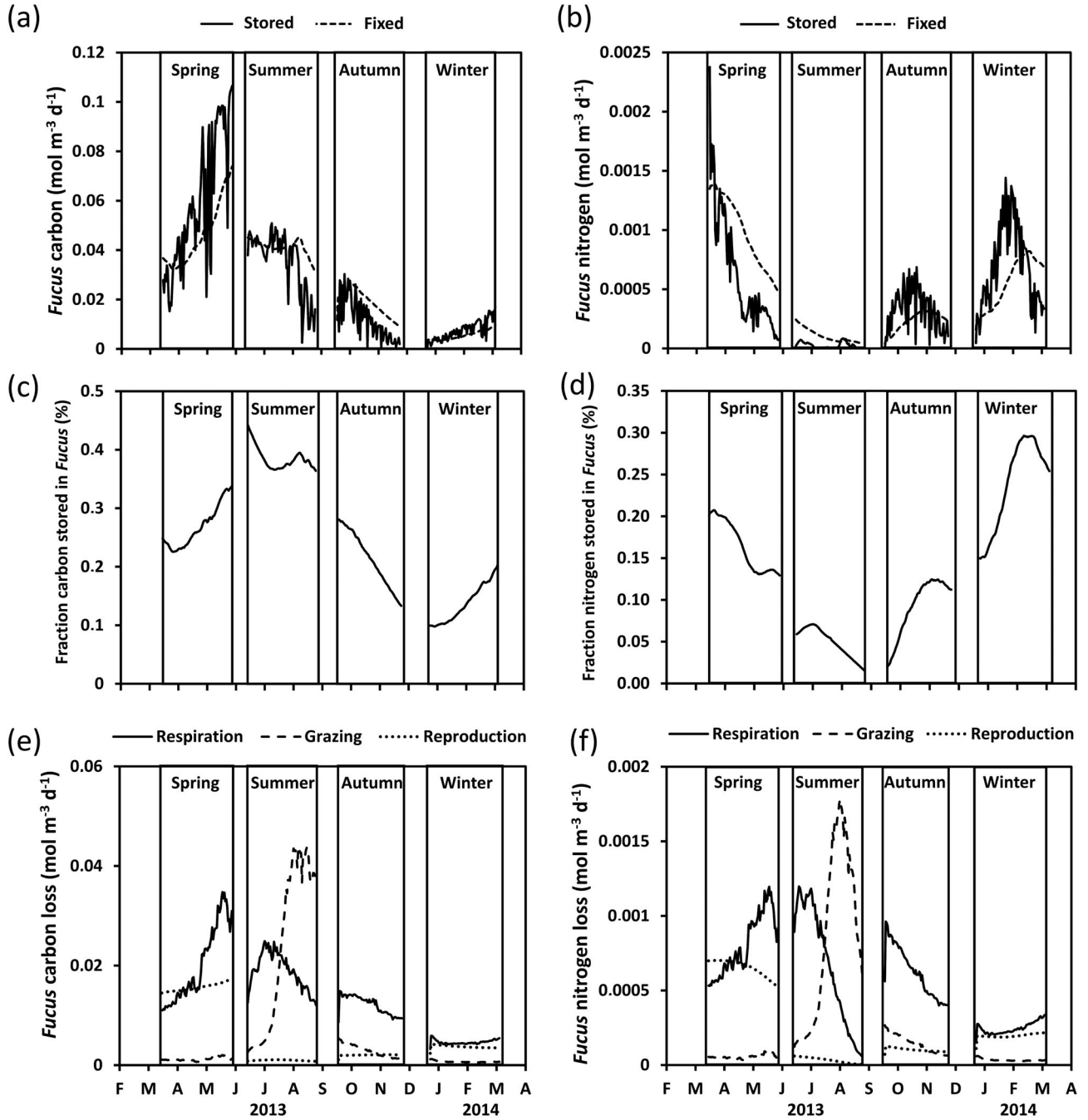


**Fig. 4.** Seasonal cycle of stored carbon (a) and nitrogen (b) used for fixation in structural components leading to *Fucus vesiculosus* growth. Simulated fractions of carbon (c) and nitrogen (d) stored in *Fucus*. Modeled loss processes due to respiration, grazing of the three mesograzers (*Idotea*, *Gammarus* and *Littorina*) and reproduction in *Fucus* carbon (e) and nitrogen (f) in the KOB, with ambient temperature and  $p\text{CO}_2$  conditions over different seasons. Seasons: spring: 04 April 2013–19 June 2013; summer: 04 July 2013–17 September 2013; autumn: 10 October 2013–18 December 2013; winter: 16 January 2014–01 April 2014.

preferences for *Fucus* or macroepiphytes. For example, for *Idotea* grazing (mol m<sup>-3</sup> d<sup>-1</sup>) on *Fucus* we used:

$$G_{I,N} = \frac{d_I \cdot \text{GR}_{I,N} \cdot G_{I,T} \cdot \text{FP}_I \cdot \text{Fucus}_N^{\text{struc}}}{F_{tN}} \quad (28)$$

and

$$G_{I,C} = \frac{d_I \cdot \text{GR}_{I,C} \cdot G_{I,T} \cdot \text{FP}_I \cdot \text{Fucus}_C^{\text{struc}}}{F_{tC}} \quad (29)$$

Corresponding equations were applied to nitrogen- and carbon-specific *Gammarus* sp. and *L. littorea* grazing on *Fucus*. However, the nitrogen and carbon loss due to grazing depends

on the maximal species-specific grazing rate of individual *Idotea* and gammarideans ( $GR_{I,N}$ ,  $GR_{G,N}$  in  $\text{mol N ind}^{-1} \text{d}^{-1}$  and  $GR_{I,C}$ ,  $GR_{G,C}$  in  $\text{mol C ind}^{-1} \text{d}^{-1}$ ; Goecker and Kåll 2003) as well as of *Littorina* ( $GR_{L,N}$  in  $\text{mol N ind}^{-1} \text{d}^{-1}$  and  $GR_{L,C}$  in  $\text{mol C ind}^{-1} \text{d}^{-1}$ ; Gutow et al. 2016) and their abundance in the KOBs ( $d_I$ ,  $d_G$ ,  $d_L$  in  $\text{ind m}^{-3}$ ; Werner et al. 2016) with species-specific food preferences ( $FP_I$ ,  $FP_G$ ,  $FP_L$ ; Goecker and Kåll 2003) for *Fucus* related to the total *Fucus* and macroepiphyte biomass ( $Ft_N$  in  $\text{mol N m}^{-3}$  and  $Ft_C$  in  $\text{mol C m}^{-3}$ ). In the KOB experiments, measured grazer abundances at the beginning and end of each experiment were interpolated using a logarithmic regression, to obtain continuous time series with daily resolution ( $d_I$ ,  $d_G$ ,  $d_L$ ). In addition, we added species-specific temperature factors ( $G_{I,T}$ ,  $G_{G,T}$ ,  $G_{L,T}$ ), accounting for the dependence of metabolic rates and thus grazing rates of the animals on temperature. Temperature dependence, for example, of *Idotea* grazing was quantified using a non-linear regression model (Blanchard et al. 1996) and range between 0 and 1.

$$G_{I,T} = \left( \frac{T_{I,\max} - T}{T_{I,\max} - T_{I,\text{opt}}} \right)^{\beta_I} \cdot e^{\left( -\beta_I \left( \frac{T_{I,\max} - T}{T_{I,\max} - T_{I,\text{opt}}} - 1 \right) \right)}, \quad (30)$$

with  $T \leq T_{I,\max}$  and  $T_{I,\text{opt}} < T_{I,\max}$ . *Idotea* grazing rate was fitted against different temperature levels (5–30°C) obtained in the laboratory for Baltic Sea *F. vesiculosus* (Gülzow 2015). Temperature dependence of *Gammarus* and *Littorina* grazing on *Fucus* was similarly determined with nonlinear regression analysis on data for grazing rate against temperature level (Gülzow 2015; Hamer and Wahl unpubl. data). Carbon and nitrogen released due to grazing processes were assumed to be directly mineralized and added to the pool of free available DIN and DIC in the KOB water.

### Herbivores and epiphytes as nutrient sinks and sources

Biomass of microepiphyte and macroepiphyte and the three main mesograzers were prescribed, that is, not explicitly represented by model state variables. The daily increase or decrease in carbon and nitrogen of epiphytes and grazers was implemented in the model as processes of nutrient release (DIC and DIN) for the system (*source*) or as epiphyte and/or grazer assimilation of nutrients fixed in their biomass (*sink*). Daily biomass differences were calculated for each prescribed biological variable. Microepiphyte and macroepiphyte were converted from units of g dry biomass to  $\text{mol N m}^{-3}$  using 0.00479 or 0.00207  $\text{mol N g}^{-1}$ , respectively, according to Pedersen and Borum (1996) and the KOB volume ( $1.47 \text{ m}^3$ ). For conversion of  $\text{mol N m}^{-3}$  to  $\text{mol C m}^{-3}$  we applied the C/N ratio of Redfield (106/16). Grazers were converted from units of g ash-free DM (AFDM) to  $\text{mol C m}^{-3}$  and then to  $\text{mol N m}^{-3}$ , applying the molar ratios of Hillebrand et al. (2009) for *Idotea* (5.41), *Gammarus* (5.07), and *Littorina* (5.64).

The model input includes constant parameters and seasonally varying external biological as well as physical parameters. The values assigned to these parameters and the sources from which they were drawn can be found in Tables 1 and 4. An effort was made to use data derived from studies on Baltic *F. vesiculosus*, epiphytes, and grazers. Due to occasional lack of data on these groups for the Baltic Sea, we also used data derived from studies on the closely related *Fucus serratus* L. and comparable epiphyte and grazer species from the North Sea.

### Model simulations

All model simulations described in this section were computed for four independent experiments, but then integrated over one growing season of 365 d beginning in spring, from

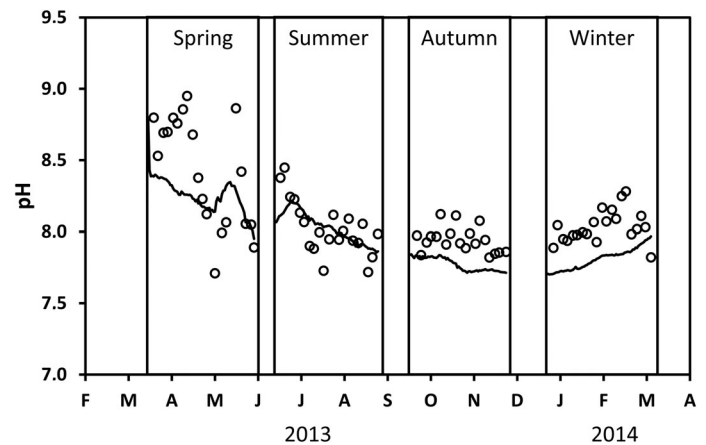


**Fig. 5.** Measured (points) and modeled (lines) pH during experiments in the KOB with ambient temperature and  $p\text{CO}_2$  conditions over different seasons. Seasons: spring: 04 April 2013–19 June 2013; summer: 04 July 2013–17 September 2013; autumn: 10 October 2013–18 December 2013; winter: 16 January 2014–01 April 2014. Data are from the pH measurements of Wahl et al. (2015).

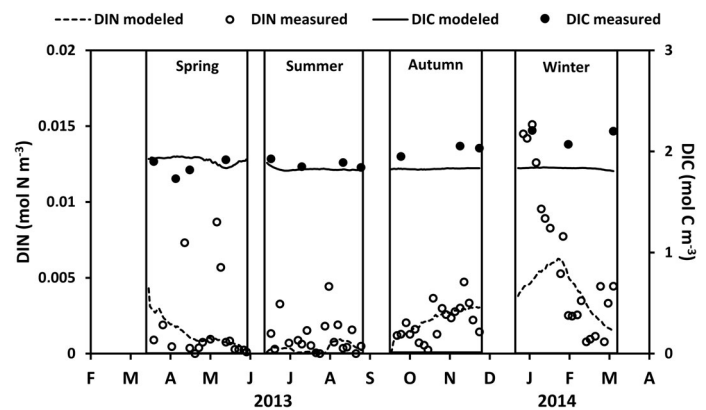


**Fig. 6.** Measured and modeled DIC and DIN during experiments in the KOB, with ambient temperature and  $p\text{CO}_2$  conditions over different seasons. Seasons: spring: 04 April 2013–19 June 2013; summer: 04 July 2013–17 September 2013; autumn: 10 October 2013–18 December 2013; winter: 16 January 2014–01 April 2014. Data are from the measurements of Wahl et al. (2015).

April 2013 to March 2014. The model was forced with realistic atmospheric, hydrographic, and dissolved-nutrient data, which were either measured during KOB experiments in the Kiel Fjord or taken from DWD, GEOMAR, and LLUR (for data sources, see Table 1). The model was developed with help of a special editor (Code Generation Tool Editor [CGT-EDIT]) for development and formal description of the model structure. The CGT generated the model code from a MATLAB template. The editor and the CGT (<http://ergom.net/index.php/code-generation-tool.html>) were developed at the Leibniz Institute for Baltic Sea Research Warnemünde. All required computations were carried out numerically with the computing software MATLAB R2017a (The MathWorks).

### Model validation: Comparison to KOB experiments

The model validation was achieved by comparing the predicted relative growth rates of *Fucus*, pH, DIC and DIN concentrations in the KOB water with the measured relative *Fucus* growth rates, pH, DIC, and DIN values in the four sequential KOB experiments under ambient abiotic conditions (Fig. 2). The experiments ran from 04 April 2013 to 19 June 2013 (spring), from 04 July 2013 to 17 September 2013 (summer), from 10 October 2013 to 18 December 2013 (autumn), and from 16 January 2014 to 01 April 2014 (winter), each lasting for at least 10 weeks. To evaluate the model performance and to measure the differences between values predicted by the model and the values actually observed, root-mean-square

**Table 6.** Sensitivity of modeled *Fucus vesiculosus* growth rates to physical, physiological and ecological parameters and initial total *Fucus* biomass as carbon (C) and nitrogen (N), quantified as the median daily percent difference between the standard and sensitivity model runs. Results are listed only for relevant parameters. Input parameters are described in Table 2.

Parameter	Variation	Spring (%)	Summer (%)	Autumn (%)	Winter (%)
Physical	$\pm 10\%$				
fr		0.03	0.3	0.1	0.1
$V_{\text{box}}$		0.1	1	1	0.4
$k_w$		0.02	0.01	0.04	0.1
$k_c$		0.1	0.1	0.2	0.1
$R_{\text{foil}}$		0.4	0.3	0.7	1
$R_{\text{KOB}}$		0.5	0.4	1	1
Physiological	$\pm 20\%$				
$\text{PAR}_{\text{opt}}$		3	3	7	10
LAI		3	3	7	10
$\mu_{\text{max}}$		19	11	11	22
$N_{\text{min}}^{\text{struc}}$		4	2	3	4
$C_{\text{min}}^{\text{struc}}$		1	1	1	3
$K_{\text{m}(\text{CO}_2)}$		0.1	0.1	0.3	1
$K_{\text{m}(\text{HCO}_3)}$		2	2	2	3
$r_0$		2	4	3	2
$\beta$		1	6	2	0.4
RE		0.3	0.04	0.1	0.3
$T_{\text{max}}$		15	3	5	30
$T_{\text{opt}}$		20	4	9	38
$\beta_F$		4	1	1	10
Ecological	$\pm 30\%$				
$A_{\text{microepi}}$		1	0.3	0.4	1
$B_{\text{microepi}}$		1	0.3	0.2	1
$A_{\text{macroepi}}$		1	1	1	2.3
$B_{\text{macroepi}}$		0.3	1	1	1
$\text{FP}_{\text{I,G,L}}$		0.4	6	1	1
$\text{GR}_{\text{I,G,L}}$		0.4	6	0.4	1
$T_{\text{I,G,L max}}$		1	3	4	4
$T_{\text{I,G,L opt}}$		2	0.4	5	5
$\beta_{\text{I,G,L}}$		1	0.4	0.3	1
Initial	$\pm 20\%$				
C and N		0.3	4	1	1



deviation (RMSD), absolute value of the percentage model bias (Pbias) and coefficient of determination ( $R^2$ ) was used for *Fucus* growth, pH, DIC, and DIN concentrations.

### Sensitivity analysis of parameter values

The values of the input parameters used for the solution of the model were drawn from physiological and ecological studies, with no calibration being performed. Nevertheless, it is useful for the evaluation of the validity of the model to test the sensitivity of its behavior against variation in these parameters. We increased the percentage by which individual parameters are varied in this sensitivity analysis from parameters representing physical ( $\pm 10\%$ ) to those representing physiological ( $\pm 20\%$ ) and ecological interactions ( $\pm 30\%$ ), corresponding to an increased complexity and lower predictability of the respective processes involved. For this purpose, a percentage of the input parameters' value is subtracted or added to them and changes in modeled *Fucus* growth are quantified. Results of the sensitivity runs were expressed as the percent difference from the standard run:

$$\% \text{Difference} = \frac{|x_{\text{standard}} - x_{\text{sensitivity}}|}{x_{\text{standard}}} \times 100, \quad (31)$$

where  $x$  is the model prediction of a given variable on a given day, "standard" refers to the standard run, and "sensitivity" refers to the sensitivity runs. Daily values of %difference were calculated separately for each season, and the overall seasonal model sensitivity to a given parameter was computed as the median of all %difference estimates across both sensitivity runs.

The sensitivity of the modeled *Fucus* growth rates to initial conditions was also tested. The model was run with  $\pm 20\%$  of the initial biomass of *Fucus* as nitrogen and carbon, as well as with variations of the proportions of carbon and nitrogen for structure and storage.

### Growth and pH simulations under different temperature and $p\text{CO}_2$ conditions

The influence of ocean warming and acidification on *Fucus* growth rates and pH of the KOB water was assessed by running the model with the ambient temperature of Kiel Fjord water and warmer water ( $+5^\circ\text{C}$  relative to Fjord water) at two  $p\text{CO}_2$  levels, ambient (ca. 400 ppm) vs. ca. 1100 ppm in the headspace above the Benthocosms. Consequently, four treatments were simulated: (1) Ambient, (2)  $+\text{CO}_2$ , (3)  $+\text{Temp}$ , and (4)  $+\text{Temp} + \text{CO}_2$ . Abiotic and biotic forcing parameters were adjusted according to the values measured during the KOB experiments. The model predictions of *Fucus* growth rates and pH of the KOB water under the different temperature and  $p\text{CO}_2$  conditions were compared to the measured growth rates and pH over the seasons. In addition, the effect of running the model with daily temperature means vs. daily maxima was

compared for *Fucus* growth under increased temperature conditions.

## Results and assessment

### Model validation

The *Fucus* length–growth rate measurements (Graiff et al. 2015b) as well as the pH, DIC, and DIN concentrations (Wahl et al. 2015b) measured during the KOB experiments provide an ideal dataset for model validation. The model reproduces both the magnitude and the seasonal growth cycle of *Fucus* in the KOB over 1 yr under ambient conditions, but with some exceptions depending on the season (Fig. 3). Maximum growth rates were simulated for the period between June

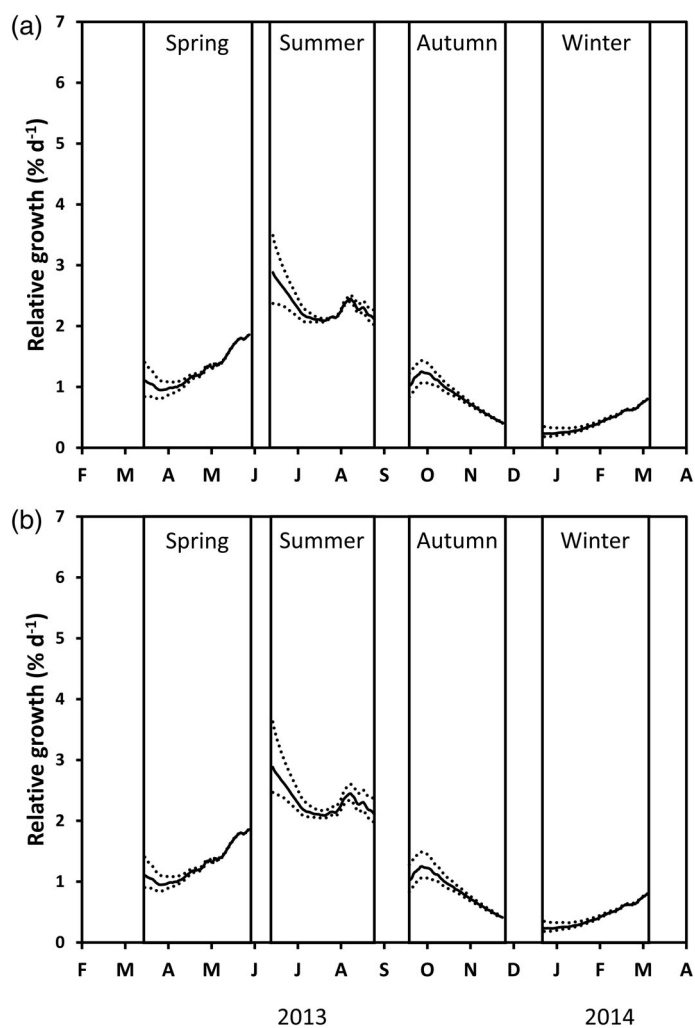


**Fig. 7.** Predicted relative growth rates of *Fucus vesiculosus* from the standard run (solid lines) and runs in which (a) stored carbon and (b) structural carbon is  $\pm 20\%$  (dotted lines) during experiments in the KOB, with ambient temperature and  $p\text{CO}_2$  conditions over different seasons. Seasons: spring: 04 April 2013–19 June 2013; summer: 04 July 2013–17 September 2013; autumn: 10 October 2013–18 December 2013; winter: 16 January 2014–01 April 2014.

and early September, with the highest values in July and a decline thereafter. Winter months (December and January) revealed the lowest growth rates, which were simulated by the model (RMSD = 0.09% d<sup>-1</sup>), however, with a slight model underestimation bias (Pbias = -13.07, Table 5). The coefficient of determination was high in winter when relating observed and modeled values ( $R^2 = 0.99$ ). However, in spring the model showed a stronger tendency to underestimate *Fucus* growth by 30–40% compared to the experiment (RMSD = 0.65% d<sup>-1</sup>, Pbias = -32.66,  $R^2 = 0.86$ ; Table 5).

An annual cycle of storage and fixation rates for carbon and nitrogen in *Fucus* (Fig. 4a,b) is simulated by the model. Comparison of the simulated fraction of stored carbon and nitrogen in *Fucus* (Fig. 4c,d) with measured carbohydrates (e.g., mannitol) as a proxy for carbon storage and nitrogen content revealed a similar seasonal pattern (Supporting Information Fig. S2).

Potential factors influencing the seasonal pattern of *Fucus* growth include carbon and nitrogen losses related to respiration, reproduction, and grazing. Their seasonal variation is depicted in Fig. 4e,f. Respiration is controlled by temperature and thus shows a peak in late spring and summer, with minimum values throughout the winter experiment. During spring and autumn, loss processes are dominated by respiration of *Fucus*. In summer, however, the model indicates that grazing is the most important loss process for *Fucus* carbon and nitrogen (Fig. 4e,f). Biomass loss due to reproduction plays a larger role only in spring, when the reproductive parts of *Fucus* are shed after release of gametes, which comprise a considerable proportion of the biomass (Graiff et al. 2017).

Predicted pH of the KOB water under ambient conditions is higher in spring compared to late autumn and winter (Fig. 5),

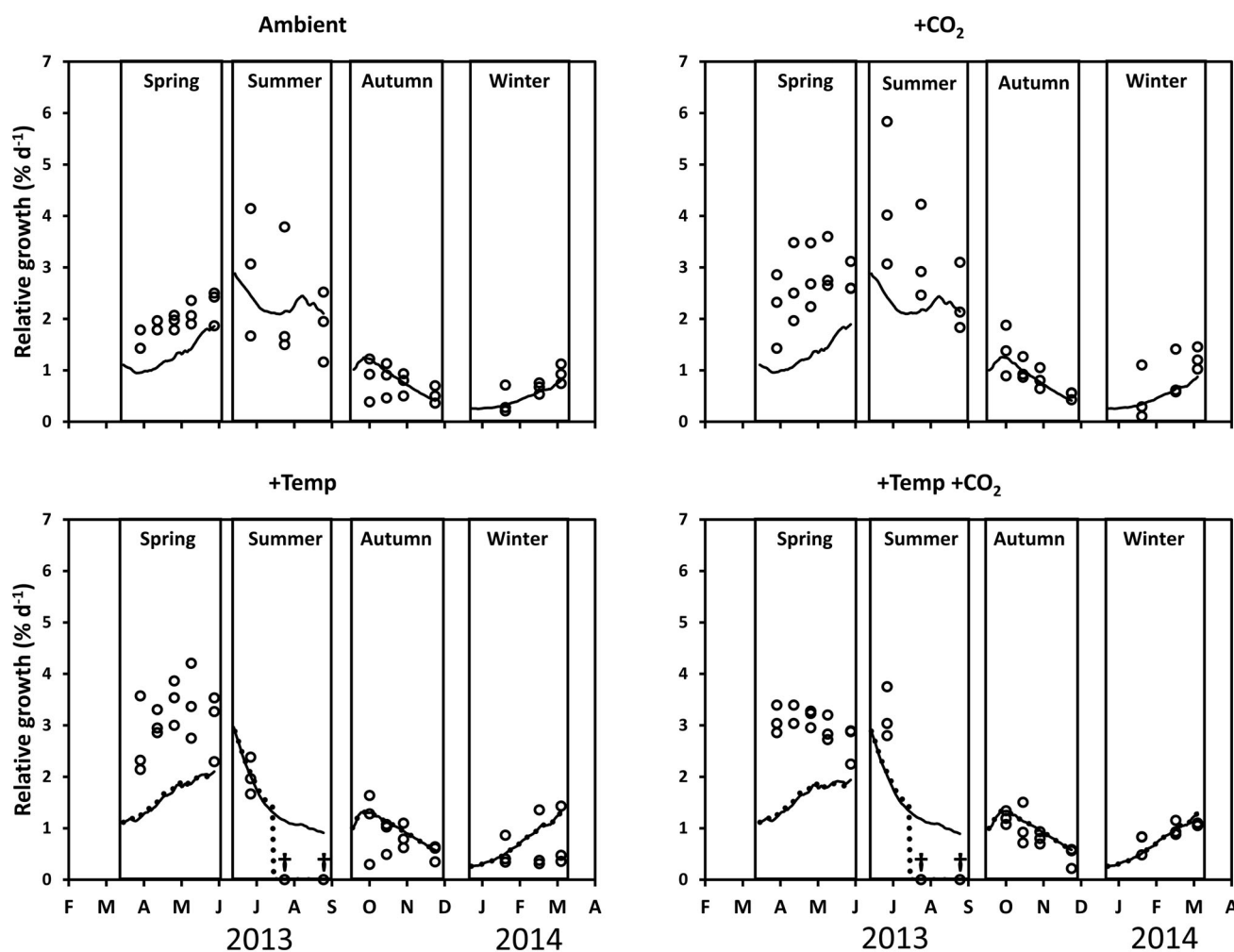


**Fig. 8.** Relative growth rates (points: measured; solid line: modeled with daily temperature means; dotted lines: modeled with daily temperature maxima) of *Fucus vesiculosus* during experiments in the KOB, with various temperature and  $p\text{CO}_2$  conditions over different seasons. Seasons: spring: 04 April 2013–19 June 2013; summer: 04 July 2013–17 September 2013; autumn: 10 October 2013–18 December 2013; winter: 16 January 2014–01 April 2014. Temperature and  $p\text{CO}_2$  conditions: Ambient: ambient temperature and  $p\text{CO}_2$ , +CO<sub>2</sub>: ambient temperature and elevated  $p\text{CO}_2$ , +Temp: elevated temperature and ambient  $p\text{CO}_2$ , +Temp +CO<sub>2</sub>: elevated temperature and  $p\text{CO}_2$ . Cross (†) indicates dieback of *F. vesiculosus* in the summer experiment under warming. Data are from the length–growth measurements of Graiff et al. (2015b).

which reproduces the magnitude and seasonal variation of measured pH during the different KOB experiments (Wahl et al. 2015b). Under ambient conditions, RMSDs between model predictions and measurements were between 0.14 and 0.36 for pH, depending on the season (Table 5). The absolute values of the Pbias indicated a slight model underestimation bias in each season for pH (Table 5).

The model reproduces both the DIC and DIN concentrations in the KOB in most seasons in a similar magnitude as the measured data, but there are several exceptions in each season (Fig. 6). DIN was underestimated by the model in spring, summer, and winter (spring: RMSD = 0.003 mol N m<sup>-3</sup>, Pbias = -39.07, R<sup>2</sup> = 0.44; summer: RMSD = 0.001 mol N m<sup>-3</sup>, Pbias = -65.09, R<sup>2</sup> = 0.74; winter: RMSD = 0.005 mol N m<sup>-3</sup>, Pbias = -33.81, R<sup>2</sup> = 0.14), as the measured DIN concentrations showed high intraseasonal variations. In contrast, in autumn, the model tends to overestimate DIN (autumn: RMSD = 0.001 mol N m<sup>-3</sup>, Pbias = 9.62, R<sup>2</sup> = 0.38). In summer, autumn, and winter, the model underestimates (summer: RMSD = 0.05 mol C m<sup>-3</sup>, Pbias = -2.49, R<sup>2</sup> = 0.01; autumn: RMSD = 0.19 mol C m<sup>-3</sup>, Pbias = -8.98, R<sup>2</sup> = 0.31; winter: RMSD = 0.34 mol C m<sup>-3</sup>, Pbias = -15.44, R<sup>2</sup> = 0.26), but in spring, the model overestimates the DIC concentration in the KOB water (spring: RMSD = 0.13 mol C m<sup>-3</sup>, Pbias = 3.87, R<sup>2</sup> = 0.01).

### Sensitivity analysis

The effect of varying individual parameter values on modeled *Fucus* growth rate is demonstrated in Table 6. The model is relatively insensitive to the range of physical parameters ( $\pm 10\%$ ) influencing the *Fucus* growth rate. The largest sensitivities are observed in response to  $\pm 20\%$  variations of the maximal growth rate ( $\mu_{\max}$ ) and the parameters ( $T_{\max}$ ,  $T_{\text{opt}}$ ,  $\beta_F$ ) of the temperature dependence of *Fucus* growth. Sensitivity to  $\pm 20\%$  variations of PAR optimum for *Fucus* growth ( $\text{PAR}_{\text{opt}}$ ) and self-shading by *Fucus* (LAI) are highest in autumn and winter, when light is limiting *Fucus* growth. Changes of  $\pm 30\%$  of values of the species-specific food preferences of the different grazer species ( $\text{FP}_1$ ,  $\text{FP}_G$ ,  $\text{FP}_L$ ) and their maximal species-specific grazing rates ( $\text{GR}_1$ ,  $\text{GR}_G$ ,  $\text{GR}_L$ ) result in changes of *Fucus* growth rate in summer (Table 6), while changes in other parameters induce much smaller changes in the modeled growth rates.

Variations by  $\pm 20\%$  of initial total *Fucus* biomass as carbon (C) and nitrogen (N) in each season result in a slight modification of the modeled growth rates in summer (Table 6). Increases and decreases ( $\pm 20\%$ ) in initial proportions of stored and structural carbon result in similar *Fucus* growth rates, with slight differences only in magnitude at the beginning of each experiment (Fig. 7).

### *Fucus* growth and pH under different temperature and pCO<sub>2</sub> conditions

The temporal development of measured and modeled *Fucus* growth follows a distinct seasonal pattern under all temperature

and pCO<sub>2</sub> conditions tested. Overall, temperature effects are more pronounced than CO<sub>2</sub> effects (Fig. 8). In spring, increased temperature results in slightly higher modeled growth rates compared to ambient conditions. However, modeled growth rates also indicate the tendency of the model to underestimate *Fucus* growth compared to the measured growth rates in spring (Pbias = -45.61; Table 5). During the summer experiment, decreasing growth rates are obvious under increased daily mean temperatures, and a die-back of *Fucus* is simulated, if daily maximum temperatures are considered (Fig. 8). In the autumn and winter experiments, modeled *Fucus* growth rates are low under the different temperature and pCO<sub>2</sub> conditions (Fig. 8). Under increased pCO<sub>2</sub> and ambient temperature, the model tends to underestimate *Fucus* growth in all seasons, which was lowest in autumn (Table 5). Increased temperature and ambient pCO<sub>2</sub> conditions lead to a model underestimation bias for *Fucus* growth in spring, but to an overestimation bias of growth in summer, autumn, and winter (Table 5). The model produces an underestimation bias in spring and summer under combined increased temperature and pCO<sub>2</sub> conditions. However, in autumn and winter the model overestimation bias was low under these conditions (Table 5). The coefficients of determination (R<sup>2</sup>) were high in summer, autumn

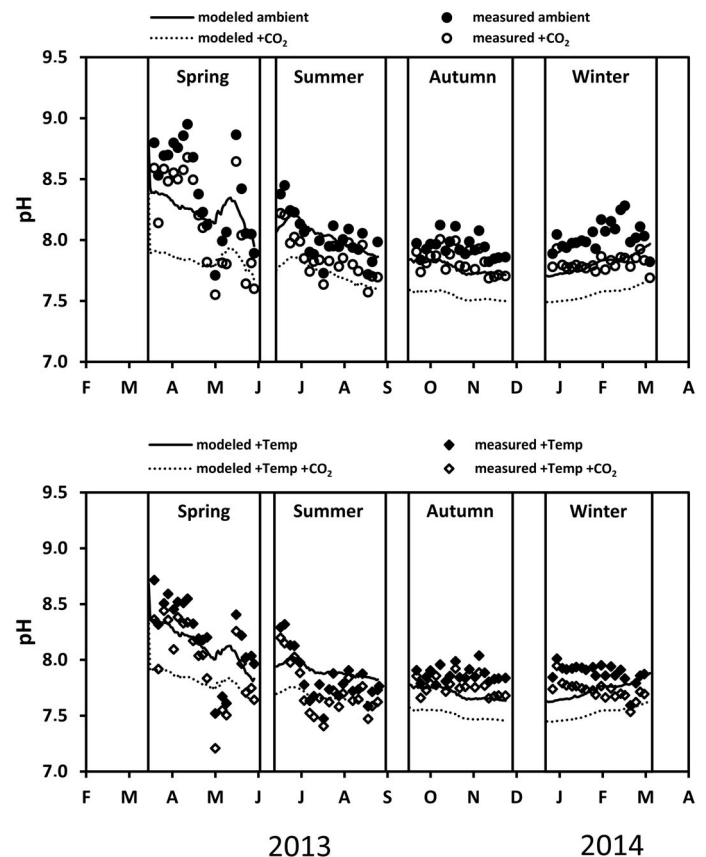


**Fig. 9.** Modeled and measured pH during experiments in the KOB, with various temperature and pCO<sub>2</sub> conditions over different seasons (see Fig. 8 for details). Data are from the pH measurements of Wahl et al. (2015).

and winter when relating observed and modeled values, but rather low in spring under all scenarios (Table 5).

Comparison of the modeled pH under increased temperature and/or  $p\text{CO}_2$  conditions in the headspace above the KOBs shows that the pH decreased due to enhanced  $p\text{CO}_2$ , reflecting natural seasonal pH variations (Fig. 9). RMSDs between model predictions and measurements were between 0.19 and 0.49 for pH depending on the season and scenario (Table 5). However, during all seasons the model slightly underestimates the pH in all treatments (Table 5), except during the summer experiment under increased temperature conditions, the model slightly overestimates the pH of the KOB water (Pbias = 0.88).

## Discussion

### General model behavior

The aim of the study was to develop a numerical box model to better understand and quantify abiotic and biotic processes and their complex interactions around the ecologically important primary producer and ecosystem engineer *F. vesiculosus*, in a nearly natural community in the KOBs. However, the model can be applied beyond the KOBs, for example, for in situ studies.

Ultimately, it is anticipated that this new model component of a “nearshore *Fucus* community” will be coupled to a three-dimensional (3D) hydrodynamic-biogeochemical model of the western Baltic Sea. This new approach may improve the representation of local nutrient dynamics in shallow coastal regions and examine the growth dynamics of *Fucus* in a more realistic environment that, for instance, includes competition with phytoplankton contributing to increasing light attenuation in the water column (see modeling approaches by Hadley et al. 2015 and van der Molen et al. 2017 for macroalgal farms). If aiming at representing in situ conditions, we might find missing processes that are not relevant in the KOBs, but perhaps are in the field, such as adaptation of *Fucus* to changing environmental factors.

The level of detail at which to pitch a model depends on its purpose. We had to make several simplifications. The aim of the present model is to realistically simulate seasonal growth of *Fucus* in the KOB and to include sufficient details such as seasonal variations in nutrient composition and concentration. This has been accomplished through the implementation of C and N reserves, leading to a temporal decoupling of nutrient assimilation and growth. This specific property is especially common in perennial macroalgal species (Chapman and Craigie 1977; Lehvo et al. 2001; Gómez and Huovinen 2012). Therefore, C and N reserves have been used in macroalgal models previously, for example, Solidoro et al. (1997), Broch and Slagstad (2012). However, the present one is the first realistic seasonal growth model for *Fucus* and similar species, as the model describes seasonal variation in N and C content reasonably well. We have explicitly included other aspects of seasonality, such as reproduction. *Fucus* loses

considerable amounts of biomass due to reproduction in spring, when the reproductive parts are shed after gamete release (Graiff et al. 2017). The model might be useful in studying such phenomena in more detail. Interactions with other biotic components of the system influencing the *Fucus*–grazer–epiphyte system were regarded important and included in the model. Indeed, the model indicates that grazing is the most important loss process of *Fucus* in summer. However, despite their quantitative importance, both grazers and epiphytes were no prognostic state variables, but were prescribed. This simplified approach was necessary, as we considered the uncertainty of the necessary parametrizations of all these processes as too high. More research to elucidate their role in the *Fucus* system is needed, to reach the level of knowledge required for modeling the responses of this ecologically important community to global change.

Most recent macroalgal-growth models have been part of quite complex ecological model systems, where the macroalgae have been included on a population level, for example, Duarte et al. (2003), Trancoso et al. (2005), and Aveytua-Alcázar et al. (2008). Compared to their relatively simple representation of macroalgae, we developed a rather complex model focused more on thorough descriptions of numerous individual physiological processes, defining seasonality and biotic interactions of adult *Fucus* growth. The model allows one to identify the most important processes (assimilation and respiration of *Fucus*, storage of nutrients in *Fucus*, self-shading and shading by epiphytes, and grazing by the different mesograzers taxa) from a quantitative point of view. However, in our model only adult individuals are considered, and not the complete life cycle of *Fucus* including motile gametes, germlings and juvenile individuals.

### Model validation and sensitivity analysis under ambient conditions

The results indicate that the model resolves seasonal *Fucus* growth and composition using realistic environmental data as input. The relative growth rate of *Fucus* increases rapidly in late spring (April to May) and reaches a maximum rate of almost  $3\% \text{ d}^{-1}$  in June/July, which is followed by a more gradual decline during summer. Later in the year, growth decreases during autumn (September to November) reaching a low rate (ca.  $0.40\% \text{ d}^{-1}$ ) in winter (December to February) before increasing again in March. This seasonal growth pattern and the magnitude of the values were measured in the KOB experiments under ambient conditions (Graiff et al. 2015b) as well as under natural conditions in shallow waters of the Kiel Fjord (Wahl et al. 2010). However, the model simulations for spring underestimated *Fucus* growth compared to experimental measurements in the KOB. This may suggest that in the model simulation, the loss terms such as respiration are too high or losses due to grazing by herbivores are not sufficiently well parametrized during spring. However, most likely this underestimation results from the inclusion of reproductive biomass loss in spring in our modeling approach, but not in

measurements of growth in the length of vegetative *Fucus* apices in the KOB experiments (Graiff et al. 2015b). During the other seasons, *Fucus* individuals do not lose considerable amounts of biomass due to reproduction (Graiff et al. 2017), which means that the modeled biomass growth rates better resemble measured length growth rates in the KOBs.

The choice of parameters and equations for storage as well as fixation in structure depends on the carbon and nitrogen data measured at the beginning of each experiment. Thereafter, the abiotic and biotic forcing factors influence the storage or fixation of nitrogen and carbon in the structural components of *Fucus*. Thus, the model simulated an accumulation of carbon (e.g., stored carbohydrates such as mannitol) in late spring and summer, when light conditions for photosynthesis are optimal but nitrogen concentrations in the water column are low. As we implemented it in the model, *Fucus* uses stored nitrogen for rapid growth and/or reproduction in this period, which corresponds with field observations (Lehvo et al. 2001).

The simulation of pH, DIC, and DIN was realistic, comparable in range and seasonal variation with observed pH values, DIC, and DIN concentrations during the KOB experiments. However, there were several exceptions in each season. Especially, the measured DIN concentrations showed high intra-seasonal variations, which were not reproduced by the model. The high variability of the measured values may be due to stochastic changes in the nutrient and carbonate systems of the Kiel Fjord, for example, due to upwelling of nutrient- and DIC-enriched deep water (Saderne et al. 2013). The implementation of a state-of-the-art carbonate system developed for the open Baltic Sea is adequate for the experimental shallow-water KOB system. The simulated air-seawater CO<sub>2</sub> surface fluxes were calculated using wind speed and empirical data (for details, see Schneider and Müller 2018). Then, the model computes the *p*CO<sub>2</sub> and the pH of the KOB water from atmospheric *p*CO<sub>2</sub>. However, to take the special situation of a limited water-surface area and the influence of the wave generator in the KOB into account, it is necessary to use very high wind speeds (15 m s<sup>-1</sup>) in our modeling approach.

The sensitivity analysis performed with the new model revealed a limited influence of a variation in shading by epiphytes on *Fucus* growth rates in all seasons. This results from the low epiphytic overgrowth on *Fucus* individuals under the ambient conditions in the KOB. This is in accordance with the study by Bokn et al. (2002), which showed that adult *Fucus* individuals appear insensitive to competition from loose-lying ephemeral macroalgae, regardless of the production levels of these macroalgae. The simulated impact of herbivory on *Fucus* growth rates was high in summer and originates mainly from its highly seasonal nature. The importance of transitory peaks in the number of herbivores, arising from unusually favorable conditions (e.g., warm summer conditions), and their effect on *Fucus* (Nilsson et al. 2004) seem to be well implemented in the model.

Different factors have been suggested to control seasonal growth of *Fucus*, some of them playing a particularly significant

role in specific areas or in particular periods in time (Supporting Information Fig. S1). Our present knowledge of physiological processes suggests that the most important factors determining growth patterns of macroalgae are light, temperature, and nutrients (Lüning 1990; Bäck and Ruuskanen 2000; Eriksson and Bergström 2005; Nygård and Dring 2008). The importance of light and temperature for *Fucus* growth is supported by the results of the sensitivity analyses performed with the new model. The model's output appears most sensitive to variations of parameters associated with light and temperature limitation (PAR<sub>opt</sub>, LAI, T<sub>max</sub> and T<sub>opt</sub>). For seasonal growth patterns of macroalgae, there is evidence that day length forces the growth rate of some species (Bartsch et al. 2008), but this has not been proven for *Fucus*. For Baltic *Fucus*, a direct relationship between nitrogen availability and storage and seasonal growth has been shown (Lehvo et al. 2001).

The correct choice of the initial proportions of stored and structural carbon or nitrogen of *Fucus* for the model results was indicated by the sensitivity analyses. In the modeling approach, the choice of parameters and equations for storage as well as fixation in *Fucus* structure is dependent on the carbon and nitrogen data measured at the beginning of each experiment. Thereafter, the abiotic and biotic forcing factors drive and modulate the nutrient storage or fixation in structural *Fucus* components. The model reproduces the annual cycle of tissue nitrogen and carbon in *Fucus* realistically, indicating that the definition of the most important abiotic and biotic processes influencing *Fucus* composition is correct.

### ***Fucus* growth under different temperature and *p*CO<sub>2</sub> conditions**

Overall, temperature effects are more pronounced than CO<sub>2</sub> effects when simulating growth of *Fucus* in the KOBs under different temperature and *p*CO<sub>2</sub> treatments. This result was previously obtained in the KOB studies (see Graiff et al. 2015b, 2017; Werner et al. 2016). However, now, having established the model, it is possible to better highlight the actual threat of increasing temperatures to the entire *Fucus*-grazer-epiphyte system in the shallow nearshore waters. The highly stochastic nature of environmental factors critical to a system's behavior and the imminent threat of climate change will push these factors near or past their current extremes. During the KOB experiments, a natural heat wave in the Kiel Fjord produced peak temperatures of 28–30°C over a period of several days in the experimental warming treatment (Graiff et al. 2015b). Using the daily temperature maxima, the model simulated a die-off of *Fucus* in summer. In contrast, when the model was forced with daily temperature averages, it simulated a decrease of *Fucus* growth in summer, but no die-off. In the face of increasing short-term extreme warming events (e.g., "marine heat waves") and number of extremely hot days (in terms of sea temperatures) in the Baltic Sea (HELCOM 2013), the inclusion of temperature maxima in the model seems adequate.

The interaction of abiotic and biotic factors in *Fucus* growth can be followed by comparing growth rates under the different temperature conditions using the model simulations. Already different temperature optima and temperature limits of three components of the system (*Fucus*, mesograzers, and epiphytes) make interpretations of the effects of global warming difficult and the model can help. The KOB experiments showed that under ambient conditions, epiphyte dominance and the competitive exclusion of *Fucus* are significantly counteracted by grazing (e.g., Hillebrand et al. 2009; Poore et al. 2012) until temperature exceeds the optimal performance temperatures of the grazers. Thus, in the summer KOB experiment, a temperature-driven collapse of grazers caused a cascading effect from the consumers to the foundation species, resulting in overgrowth of *Fucus* thalli by epiphytes and finally leading to *Fucus* die-off (Werner et al. 2016). The *Fucus* model was partially able to show this *Fucus*–epiphyte–mesograzer interaction. However, as both epiphyte and grazers were prescribed, the model results need to be interpreted with caution. Nevertheless, it highlights the model's ability to capture this important ecological interaction.

During the spring KOB experiment, warming by 5°C increased the growth of *Fucus* length by almost 40% (Graiff et al. 2015b). This observed growth enhancement is not resolved by the model at the same magnitude compared to ambient conditions. This underestimation most likely points to the importance of reproductive biomass losses during the spring experiment. In addition, under warming, the parameters chosen for shading by epiphytes and the resulting light limitation for *Fucus* growth may be too high in spring. Interpolation of the microepiphyte and macroepiphyte DM data at the beginning and end of each experiment may lead to overestimating the effect of epiphytes on *Fucus* growth.

Under ambient and warmer temperature conditions, enhanced CO<sub>2</sub> slightly increased the growth of *Fucus* over the course of the spring experiment (Graiff et al. 2015b). This is in accordance with previous studies that observed increased biomass production in aquatic autotrophic communities under elevated pCO<sub>2</sub> (e.g., Connell and Russell 2010; Kroeker et al. 2013). The model, however, does not simulate increased *Fucus* growth and the suggested fertilizing effect of elevated pCO<sub>2</sub>. This may indicate that the implemented Michaelis–Menten parametrization of CO<sub>2</sub> and bicarbonate (HCO<sub>3</sub><sup>-</sup>) uptake is not sufficient for a comprehensive modeling of carbon assimilation by macroalgae. Especially, the determination of the implemented half-saturation constants for CO<sub>2</sub> and HCO<sub>3</sub><sup>-</sup> seems to be very variable (Sand-Jensen and Gordon 1984) and requires further investigation for better parametrization.

### Conclusions and improvements

Our model is a suitable scientific tool capable of integrating the current state of knowledge on abiotic and biotic interactions around the ecologically important primary producer and

ecosystem engineer *F. vesiculosus*, to predict its growth in the KOB in a nearly natural community. Thus, the main physiological characteristics and interactions affecting *Fucus*, indicated by the general literature and our KOB and laboratory experiments, have provided a rational basis for selecting the state variables, the structure of the model, and a first set of values for the parameters. The framework and basic principles of this parameterization and modeling effort are rather general and could be easily implemented elsewhere, provided that the required knowledge of the functioning of the system's components is available.

The *Fucus* box model developed here already provides an adequate framework to study macrophyte–grazer–epiphyte interactions, although with some limitations. In the current modeling approach, the influence of grazers and epiphytes on *Fucus* growth rate is based on abundances and biomasses measured during the KOB experiments, that is, these prescribed data were not prognostic variables. This simplified approach was necessary, as we considered the uncertainty of the necessary parametrizations of all these processes as too high. However, in this way we were able to investigate whether all relevant processes influencing seasonal *Fucus* growth are included. In a future refinement of the box model, grazers and epiphytes could be implemented as explicitly modeled state variables as well. For instance, grazers would then be capable of responding directly to changes in *Fucus* and/or epiphyte biomass or abiotic environmental changes (e.g., temperature increase). In order to improve the model for simulation of epiphyte and grazer populations associated with *Fucus*, it is recommended to undertake laboratory experiments and field surveys, to gather detailed information on environmental conditions influencing grazer and epiphyte population dynamics. For a realistic modeling of grazer populations influencing *Fucus* and epiphytes, the dependence of birth rates on per-capita feeding rates, reproduction, and mortality must be parametrized and implemented.

As the model is validated for the KOB conditions, we are now able to simulate various experimental scenarios, for example, lowered/enhanced nutrient concentrations, hypoxia events, and doubled grazer/epiphyte biomasses/numbers, which may allow one to derive KOB experiments from the model results. The effects of predicted global change, which include, especially for the Baltic Sea (BACC 2008; BACC2 2015), increasing temperatures, stronger winds in coastal areas, freshwater runoff, and progressing eutrophication, but declining salinity, may play a role in the future development of *Fucus* vegetation (Kraufvelin et al. 2012; Takolander et al. 2017). We are optimistic that our modeling approach can help to predict and evaluate these effects on the *Fucus* system in the Baltic Sea.

Future improvements to our model may include the frond morphology, 3D structure, and multicellularity of *Fucus*. In our model approach, we have not considered frond morphology. Thus, we have made no distinction between newly

formed tissue and old tissue, although the differences can be considerable (Sjøtun 1993; Sjøtun and Gunnarsson 1995); but this might be included as well, for instance, by dividing the frond into meristematic and apical zones. Since the 3D and continually changing structure of macrophytes may be an important feature of a benthic macrophyte model, the utilization and adaptation of terrestrial tree crown (e.g., Fourcaud et al. 2008) and/or marine coral growth models (Merks et al. 2003) for modeling this structural component would be useful.

Another improvement would be the implementation of a water-movement effect on the frond erosion rate and frond mortality. The erosion of fronds may have a substantial influence on nutrient dynamics in shallow coastal regions. For instance, the majority of kelp biomass (as particulate organic carbon) is exported to adjacent habitats (Duarte et al. 2005) or even to the deep sea (Krause-Jensen and Duarte 2016). However, few data are presently available for Baltic *Fucus* on this topic. Therefore, a description and parametrization of frond erosion/breakage should also be attempted.

In the future, we intend to include our model in a fully coupled 3D hydrodynamic–biogeochemical model of the region. Technically this extension can be accomplished smoothly, as the developed *Fucus* model system can be coupled not only to a 0D box model but also to 1D or 3D circulation models. We are convinced that implementing benthic macroalgal systems will considerably improve simulation of nutrient dynamics in the nearshore waters.

## References

- Aldridge, J. N., and M. Trimmer. 2009. Modelling the distribution and growth of “problem” green seaweed in the Medway estuary, UK. *Hydrobiologia* **629**: 107–122. doi:10.1007/s10750-009-9760-6
- Alexandridis, N., A. Oschlies, and M. Wahl. 2012. Modeling the effects of abiotic and biotic factors on the depth distribution of *Fucus vesiculosus* in the Baltic Sea. *Mar. Ecol. Prog. Ser.* **463**: 59–72. doi:10.3354/meps09856
- Anders, K., and H. Möller. 1983. Seasonal fluctuations in macrobenthic fauna of the *Fucus* belt in Kiel Fjord (western Baltic Sea). *Helgol. Meeresunters.* **36**: 277–283. doi:10.1007/BF01983631
- Aneer, G., G. Florell, U. Kautsky, S. Nellbring, and L. Sjöstedt. 1983. *In-situ* observations of Baltic herring (*Clupea harengus membras*) spawning behaviour in the Askö-Landsort area, northern Baltic proper. *Mar. Biol.* **74**: 105–110. doi:10.1007/BF00413912
- Aveytua-Alcázar, L., V. F. Camacho-Ibar, A. J. Souza, J. I. Allen, and R. Torres. 2008. Modelling *Zostera marina* and *Ulva* spp. in a coastal lagoon. *Ecol. Model.* **218**: 354–366. doi:10.1016/j.ecolmodel.2008.07.019
- BACC Author Team. 2008. Assessment of climate change for the Baltic Sea Basin. Berlin: Springer-Verlag.
- BACC II Author Group. 2015. Second assessment of climate change for the Baltic Sea Basin. Heidelberg: Springer.
- Bäck, S., and A. Ruuskanen. 2000. Distribution and maximum growth depth of *Fucus vesiculosus* along the Gulf of Finland. *Mar. Biol.* **136**: 303–307. doi:10.1007/s002270050688
- Badger, M. 2003. The roles of carbonic anhydrases in photosynthetic CO<sub>2</sub> concentrating mechanisms. *Photosynth. Res.* **77**: 83–94. doi:10.1023/A:1025821717773
- Bartsch, I., and others. 2008. The genus *Laminaria sensu lato*: recent insights and developments. *Eur. J. Phycol.* **43**: 1–86. doi:10.1080/09670260701711376
- Best, E. P. H., C. P. Buzzelli, S. M. Bartell, R. L. Wetzel, W. A. Boyd, R. D. Doyle, and K. R. Campbell. 2001. Modeling submerged macrophyte growth in relation to underwater light climate: Modeling approaches and application potential. *Hydrobiologia* **444**: 43–70. doi:10.1023/A:1017564632427
- Blanchard, G. F., J.-M. Guarini, P. Richard, P. Gros, and F. Mornet. 1996. Quantifying the short-term temperature effect on light-saturated photosynthesis of intertidal microphytobenthos. *Mar. Ecol. Prog. Ser.* **134**: 309–313. doi:10.3354/meps134309
- Bokn, T. L., and others. 2002. Are rocky shore ecosystems affected by nutrient-enriched seawater? Some preliminary results from a mesocosm experiment. *Hydrobiologia* **484**: 167–175. doi:10.1023/A:1021365307438
- Brenchley, J. L., J. A. Raven, and A. M. Johnston. 1996. A comparison of reproductive allocation and reproductive effort between semelparous and iteroparous fucooids (Fucales, Phaeophyta). *Hydrobiologia* **326**: 185–190. doi:10.1007/BF00047805
- Broch, O. J., and D. Slagstad. 2012. Modelling seasonal growth and composition of the kelp *Saccharina latissima*. *J. Appl. Phycol.* **24**: 759–776. doi:10.1007/s10811-011-9695-y
- Brush, M., and S. W. Nixon. 2002. Direct measurements of light attenuation by epiphytes on eelgrass *Zostera marina*. *Mar. Ecol. Prog. Ser.* **238**: 73–79. doi:10.3354/meps238073
- Brush, M. J., and S. W. Nixon. 2010. Modeling the role of macroalgae in a shallow sub-estuary of Narragansett Bay, RI (USA). *Ecol. Model.* **221**: 1065–1079. doi:10.1016/j.ecolmodel.2009.11.002
- Buzzelli, C. P., R. L. Wetzel, and M. B. Meyers. 1999. A linked physical and biological framework to assess biogeochemical dynamics in a shallow estuarine ecosystem. *Estuar. Coast. Shelf Sci.* **49**: 829–851. doi:10.1006/ecss.1999.0556
- Cerco, C., and M. Noel. 2004. The 2002 Chesapeake Bay eutrophication model. E.P.A. 903-R-04-004, Chesapeake Bay program. Annapolis, MD: U.S. Environmental Protection Agency, p. 349.
- Chapman, A. R. O., and J. S. Craigie. 1977. Seasonal growth in *Laminaria longicruris*: Relations with dissolved inorganic nutrients and internal reserves of nitrogen. *Mar. Biol.* **40**: 197–205. doi:10.1007/BF00390875
- Connell, S. D., and B. D. Russell. 2010. The direct effects of increasing CO<sub>2</sub> and temperature on non-calcifying

- organisms: increasing the potential for phase shifts in kelp forests. *Proc. R. Soc. B Biol. Sci.* **277**: 1409–1415. doi:[10.1098/rspb.2009.2069](https://doi.org/10.1098/rspb.2009.2069)
- Cyr, H., and M. L. Pace. 1993. Magnitude and patterns of herbivory in aquatic and terrestrial ecosystems. *Nature* **361**: 148–150. doi:[10.1038/361148a0](https://doi.org/10.1038/361148a0)
- Dickson, A. G., and F. J. Millero. 1987. A comparison of the equilibrium- constants for the dissociation of carbonic-acid in seawater media. *Deep-Sea Res A Oceanograph. Res. Pap.* **34**: 1733–1743. doi:[10.1016/0198-0149\(87\)90021-5](https://doi.org/10.1016/0198-0149(87)90021-5)
- Duarte, C. M. 1992. Nutrient concentration of aquatic plants: Patterns across species. *Limnol. Oceanogr.* **37**: 882–889. doi:[10.4319/lo.1992.37.4.0882](https://doi.org/10.4319/lo.1992.37.4.0882)
- Duarte, C. M., J. J. Middelburg, and N. Caraco. 2005. Major role of marine vegetation on the oceanic carbon cycle. *Biogeosciences* **2**: 1–8. doi:[10.5194/bg-2-1-2005](https://doi.org/10.5194/bg-2-1-2005)
- Duarte, P., and J. G. Ferreira. 1997. A model for the simulation of macroalgal population dynamics and productivity. *Ecol. Model.* **98**: 199–214. doi:[10.1016/S0304-3800\(96\)01915-1](https://doi.org/10.1016/S0304-3800(96)01915-1)
- Duarte, P., R. Meneses, A. J. S. Hawkins, M. Zhu, J. Fang, and J. Grant. 2003. Mathematical modelling to assess the carrying capacity for multi-species culture within coastal waters. *Ecol. Model.* **168**: 109–143. doi:[10.1016/S0304-3800\(03\)00205-9](https://doi.org/10.1016/S0304-3800(03)00205-9)
- Elken, J., A. Lehmann, and K. Myrberg. 2015. Recent change-marine circulation and stratification, p. 131–144. *In* The BACC II Author Team [ed.], Second assessment of climate change for the Baltic Sea Basin. Springer International Publishing.
- Engkvist, R., T. Malm, and S. Tobiasson. 2000. Density dependent grazing effects of the isopod *Idotea baltica* Pallas on *Fucus vesiculosus* L in the Baltic Sea. *Aquat. Ecol.* **34**: 253–260. doi:[10.1023/A:1009919526259](https://doi.org/10.1023/A:1009919526259)
- Eriksson, B. K., and L. Bergström. 2005. Local distribution patterns of macroalgae in relation to environmental variables in the northern Baltic Proper. *Estuar. Coast. Shelf Sci.* **62**: 109–117. doi:[10.1016/j.ecss.2004.08.009](https://doi.org/10.1016/j.ecss.2004.08.009)
- Fennel, W., and T. Neumann. 1996. The mesoscale variability of nutrients and plankton as seen in a coupled model. *Ger. J. Hydrogr.* **48**: 49–71. doi:[10.1007/BF02794052](https://doi.org/10.1007/BF02794052)
- Fong, P., T. C. Foin, and J. B. Zedler. 1994. A simulation model of lagoon algae based on nitrogen competition and internal storage. *Ecol. Monogr.* **64**: 225–247. doi:[10.2307/2937042](https://doi.org/10.2307/2937042)
- Fourcaud, T., X. Zhang, A. Stokes, H. Lambers, and C. Körner. 2008. Plant growth modelling and applications: the increasing importance of plant architecture in growth models. *Ann. Bot.* **101**: 1053–1063. doi:[10.1093/aob/mcn050](https://doi.org/10.1093/aob/mcn050)
- Giordano, M., J. Beardall, and J. A. Raven. 2005. CO<sub>2</sub> concentrating mechanisms in algae: mechanisms, environmental modulation, and evolution. *Annu. Rev. Plant Biol.* **56**: 99–131. doi:[10.1146/annurev.arplant.56.032604.144052](https://doi.org/10.1146/annurev.arplant.56.032604.144052)
- Goecker, M. E., and S. E. Käll. 2003. Grazing preferences of marine isopods and amphipods on three prominent algal species of the Baltic Sea. *J. Sea Res.* **50**: 309–314. doi:[10.1016/j.seares.2003.04.003](https://doi.org/10.1016/j.seares.2003.04.003)
- Gómez, I., and P. Huovinen. 2012. Morpho-functionality of carbon metabolism in seaweeds, p. 25–46. *In* C. Wiencke and K. Bischof [eds.], Seaweed biology: Novel insights into ecophysiology, ecology and utilization. Berlin: Springer.
- Graiff, A., D. Liesner, U. Karsten, and I. Bartsch. 2015a. Temperature tolerance of western Baltic Sea *Fucus vesiculosus*—growth, photosynthesis and survival. *J. Exp. Mar. Biol. Ecol.* **471**: 8–16. doi:[10.1016/j.jembe.2015.05.009](https://doi.org/10.1016/j.jembe.2015.05.009)
- Graiff, A., I. Bartsch, W. Ruth, M. Wahl, and U. Karsten. 2015b. Season exerts differential effects of ocean acidification and warming on growth and carbon metabolism of the seaweed *Fucus vesiculosus* in the western Baltic Sea. *Front. Mar. Sci.* **2**: 1–18. doi:[10.3389/fmars.2015.00112](https://doi.org/10.3389/fmars.2015.00112)
- Graiff, A., M. Dankworth, M. Wahl, U. Karsten, and I. Bartsch. 2017. Seasonal variations of *Fucus vesiculosus* fertility under ocean acidification and warming in the western Baltic Sea. *Bot. Mar.* **60**: 239–255. doi:[10.3758/s13423-015-0974-5](https://doi.org/10.3758/s13423-015-0974-5)
- Gülzow, E. 2015. Studies on the influence of temperature on the feeding rates of important mesograzers in the western Baltic Sea. Master thesis. Univ. of Oldenburg.
- Gutow, L., A. Eckerlebe, L. Gime, and R. Saborowski. 2016. Experimental evaluation of seaweeds as a vector for microplastics into marine food webs. *Environ. Sci. Technol.* **50**: 915–923. doi:[10.1021/acs.est.5b02431](https://doi.org/10.1021/acs.est.5b02431)
- Hadley, S., K. Wild-Allen, C. Johnson, and C. Macleod. 2015. Modeling macroalgae growth and nutrient dynamics for integrated multi-trophic aquaculture. *J. Appl. Phycol.* **27**: 901–916. doi:[10.1007/s10811-014-0370-y](https://doi.org/10.1007/s10811-014-0370-y)
- HELCOM. 2013. Climate change in the Baltic Sea Area. HELCOM thematic assessment in 2013. *In* Baltic Sea environment proceedings no. 137. Washington, DC: Helsinki Commission.
- Hepburn, C. D., D. W. Pritchard, C. E. Cornwall, R. J. Mcleod, J. Beardall, J. A. Raven, and C. L. Hurd. 2011. Diversity of carbon use strategies in a kelp forest community: Implications for a high CO<sub>2</sub> ocean. *Glob. Chang. Biol.* **17**: 2488–2497. doi:[10.1111/j.1365-2486.2011.02411.x](https://doi.org/10.1111/j.1365-2486.2011.02411.x)
- Hillebrand, H., B. Worm, and H. K. Lotze. 2000. Marine microbenthic community structure related by nitrogen loading and grazing pressure. *Mar. Ecol. Prog. Ser.* **204**: 27–38. doi:[10.3354/meps204027](https://doi.org/10.3354/meps204027)
- Hillebrand, H., L. Gamfeldt, P. R. Jonsson, and B. Matthiessen. 2009. Consumer diversity indirectly changes prey nutrient content. *Mar. Ecol. Prog. Ser.* **380**: 33–41. doi:[10.3354/meps07937](https://doi.org/10.3354/meps07937)
- Hoegh-Guldberg, O., and J. F. Bruno. 2010. The impact of climate change on the world's marine ecosystem. *Science* **328**: 1523–1528. doi:[10.1126/science.1189930](https://doi.org/10.1126/science.1189930)
- Jacovides, C. P., F. S. Tymvios, D. N. Asimakopoulos, K. M. Theofilou, and S. Pashiardes. 2003. Global photosynthetically active radiation and its relationship with global solar



- radiation in the Eastern Mediterranean basin. *Theor. Appl. Climatol.* **74**: 227–233. doi:[10.1007/s00704-002-0685-5](https://doi.org/10.1007/s00704-002-0685-5)
- Johnston, A. M., and J. A. Raven. 1990. Effects of culture in high CO<sub>2</sub> on the photosynthetic physiology of *Fucus serratus*. *Eur. J. Phycol.* **25**: 75–82. doi:[10.1080/00071619000650071](https://doi.org/10.1080/00071619000650071)
- Jormalainen, V., T. Honkanen, and N. Heikkilä. 2001. Feeding preferences and performance of a marine isopod on seaweed hosts: Cost of habitat specialization. *Mar. Ecol. Prog. Ser.* **220**: 219–230. doi:[10.3354/meps220219](https://doi.org/10.3354/meps220219)
- Jormalainen, V., S. A. Wikström, and T. Honkanen. 2008. Fouling mediates grazing: Intertwining of resistances to multiple enemies in the brown alga *Fucus vesiculosus*. *Oecologia* **155**: 559–569. doi:[10.1007/s00442-007-0939-0](https://doi.org/10.1007/s00442-007-0939-0)
- Kautsky, H., L. Kautsky, N. Kautsky, U. Kautsky, and C. Lindblad. 1992. Studies on the *Fucus vesiculosus* community in the Baltic Sea, p. 33–48. In I. Wallentinus and P. Snoeijs [eds.], *Phycological studies of Nordic coastal waters*. Acta Phytogeographica Suecica, ISSN 0084-5914; 78 P.
- Kerby, N. W., and J. A. Raven. 1985. Transport and fixation of inorganic carbon by marine algae. *Adv. Bot. Res.* **11**: 71–123. doi:[10.1016/S0065-2296\(08\)60169-X](https://doi.org/10.1016/S0065-2296(08)60169-X)
- Korpinen, S., T. Honkanen, O. Vesakoski, A. Hemmi, R. Koivikko, J. Lopenen, and V. Jormalainen. 2007. Macroalgal communities face the challenge of changing biotic interactions: Review with focus on the Baltic Sea. *Ambio* **36**: 203–211. doi:[10.1579/0044-7447\(2007\)36\[203:mcftco\]2.0.co;2](https://doi.org/10.1579/0044-7447(2007)36[203:mcftco]2.0.co;2)
- Kraufvelin, P., and S. Salovius. 2004. Animal diversity in Baltic rocky shore macroalgae: can *Cladophora glomerata* compensate for lost *Fucus vesiculosus*? *Estuar. Coast. Shelf Sci.* **61**: 369–378. doi:[10.1016/j.ecss.2004.06.006](https://doi.org/10.1016/j.ecss.2004.06.006)
- Kraufvelin, P., A. T. Ruuskanen, S. Bäck, and G. Russell. 2012. Increased seawater temperature and light during early springs accelerate receptacle growth of *Fucus vesiculosus* in the northern Baltic proper. *Mar. Biol.* **159**: 1795–1807. doi:[10.1007/s00227-012-1970-1](https://doi.org/10.1007/s00227-012-1970-1)
- Krause-Jensen, D., and C. M. Duarte. 2016. Substantial role of macroalgae in marine carbon sequestration. *Nat. Geosci.* **9**: 737–742. doi:[10.1038/ngeo2790](https://doi.org/10.1038/ngeo2790)
- Kroeker, K. J., R. L. Kordas, R. Crim, I. E. Hendriks, L. Ramajo, G. S. Singh, C. M. Duarte, and J. P. Gattuso. 2013. Impacts of ocean acidification on marine organisms: quantifying sensitivities and interaction with warming. *Glob. Chang. Biol.* **19**: 1884–1896. doi:[10.1111/gcb.12179](https://doi.org/10.1111/gcb.12179)
- Lauringson, V., and J. Kotta. 2006. Influence of the thin drift algal mats on the distribution of macrozoobenthos in Kõiguste Bay, NE Baltic Sea. *Hydrobiologia* **554**: 97–105. doi:[10.1007/s10750-005-1009-4](https://doi.org/10.1007/s10750-005-1009-4)
- Lehvo, A., S. Bäck, and M. Kiirikki. 2001. Growth of *Fucus vesiculosus* L. (Phaeophyta) in the Northern Baltic Proper: energy and nitrogen storage in seasonal environment. *Bot. Mar.* **44**: 345–350. doi:[10.1515/BOT.2001.044](https://doi.org/10.1515/BOT.2001.044)
- Lüning, K. 1969. Standing crop and leaf area index of the sublittoral *Laminaria* species near Helgoland. *Mar. Biol.* **3**: 282–286. doi:[10.1007/BF00360961](https://doi.org/10.1007/BF00360961)
- Lüning, K. 1990. *Seaweeds: their environment, biogeography and ecophysiology*. New York: John Wiley and Sons.
- Markager, S., and K. Sand-Jensen. 1992. Light requirements and depth zonation of marine macroalgae. *Mar. Ecol. Prog. Ser.* **88**: 83–92. doi:[10.3354/meps088083](https://doi.org/10.3354/meps088083)
- Martins, I., and J. C. Marques. 2002. A model for the growth of opportunistic macroalgae (*Enteromorpha* sp.) in tidal estuaries. *Estuar. Coast. Shelf Sci.* **55**: 247–257. doi:[10.1006/ecss.2001.0900](https://doi.org/10.1006/ecss.2001.0900)
- Merks, R., A. Hoekstra, J. Kaandorp, and P. Sloom. 2003. Models of coral growth: spontaneous branching, compactification and the Laplacian growth assumption. *J. Theor. Biol.* **224**: 153–166. doi:[10.1016/S0022-5193\(03\)00140-1](https://doi.org/10.1016/S0022-5193(03)00140-1)
- Middelboe, A. L., K. Sand-Jensen, and T. Binzer. 2006. Highly predictable photosynthetic production in natural macroalgal communities from incoming and absorbed light. *Oecologia* **150**: 464–476. doi:[10.1007/s00442-006-0526-9](https://doi.org/10.1007/s00442-006-0526-9)
- Millero, F. J. 2010. Carbonate constants for estuarine waters. *Mar. Freshw. Res.* **61**: 139–142. doi:[10.1071/MF09254](https://doi.org/10.1071/MF09254)
- Morel, A., and R. C. Smith. 1974. Relation between total quanta and total energy for aquatic photosynthesis. *Limnol. Oceanogr.* **19**: 591–600. doi:[10.4319/lo.1974.19.4.0591](https://doi.org/10.4319/lo.1974.19.4.0591)
- Müller, J. D., B. Schneider, and G. Rehder. 2016. Long-term alkalinity trends in the Baltic Sea and their implications for CO<sub>2</sub>-induced acidification. *Limnol. Oceanogr.* **61**: 1984–2002. doi:[10.1002/lno.10349](https://doi.org/10.1002/lno.10349)
- Neumann, T., H. Siegel, and M. Gerth. 2015. A new radiation model for Baltic Sea ecosystem modelling. *J. Mar. Syst.* **152**: 83–91. doi:[10.1016/j.jmarsys.2015.08.001](https://doi.org/10.1016/j.jmarsys.2015.08.001)
- Nilsson, J., R. Engkvist, and L. E. Persson. 2004. Long-term decline and recent recovery of *Fucus* populations along the rocky shores of southeast Sweden, Baltic Sea. *Aquat. Ecol.* **38**: 587–598. doi:[10.1007/s10452-004-5665-7](https://doi.org/10.1007/s10452-004-5665-7)
- Nygård, C. A., and M. J. Dring. 2008. Influence of salinity, temperature, dissolved inorganic carbon and nutrient concentration on the photosynthesis and growth of *Fucus vesiculosus* from the Baltic and Irish Seas. *Eur. J. Phycol.* **43**: 253–262. doi:[10.1080/09670260802172627](https://doi.org/10.1080/09670260802172627)
- Omstedt, A., and others. 2012. Future changes in the Baltic Sea acid base (pH) and oxygen balances. *Tellus* **64**: 19586. <https://doi.org/10.3402/tellusb.v64i0.19586>
- Pedersen, M. F., and J. Borum. 1996. Nutrient control of algal growth in estuarine waters. Nutrient limitation and the importance of nitrogen requirements and nitrogen storage among phytoplankton and species of macroalgae. *Mar. Ecol. Prog. Ser.* **142**: 261–272. doi:[10.3354/meps142261](https://doi.org/10.3354/meps142261)
- Poore, A. G. B., and others. 2012. Global patterns in the impact of marine herbivores on benthic primary producers. *Ecol. Lett.* **15**: 912–922. doi:[10.1111/j.1461-0248.2012.01804.x](https://doi.org/10.1111/j.1461-0248.2012.01804.x)

- Port, A., K. R. Bryan, C. A. Pilditch, D. P. Hamilton, and K. Bischof. 2015. Algebraic equilibrium solution of tissue nitrogen quota in algae and the discrepancy between calibrated parameters and physiological properties. *Ecol. Model.* **312**: 281–291. doi:10.1016/j.ecolmodel.2015.05.034
- Raven, J. A., M. Giordano, J. Beardall, and S. C. Maberly. 2011. Algal and aquatic plant carbon concentrating mechanisms in relation to environmental change. *Photosynth. Res.* **109**: 281–296. doi:10.1007/s11120-011-9632-6
- Ren, J. S., N. G. Barr, K. Scheuer, D. R. Schiel, and J. Zeldis. 2014. A dynamic growth model of macroalgae: Application in an estuary recovering from treated wastewater and earthquake-driven eutrophication. *Estuar. Coast. Shelf Sci.* **148**: 59–69. doi:10.1016/j.ecss.2014.06.014
- Robertson, B. L. 1987. Reproductive ecology and canopy structure of *Fucus spiralis* L. *Bot. Mar.* **30**: 475–482. doi:10.1515/botm.1987.30.6.475
- Rönnbäck, P., N. Kautsky, L. Pihl, M. Troell, T. Söderqvist, and H. Wennhage. 2007. Ecosystem goods and services from Swedish coastal habitats: Identification, valuation, and implications of ecosystem shifts. *Ambio* **36**: 534–544. doi:10.1579/0044-7447(2007)36[534:EGASFS]2.0.CO;2
- Saderne, V., P. Fietzek, and P. M. J. Herman. 2013. Extreme variations of pCO<sub>2</sub> and pH in a macrophyte meadow of the Baltic Sea in summer: evidence of the effect of photosynthesis and local upwelling. *PLoS One* **8**: e62689. doi:10.1371/journal.pone.0062689
- Sand-Jensen, K., and D. M. Gordon. 1984. Differential ability of marine and freshwater macrophytes to utilize HCO<sub>3</sub><sup>-</sup> and CO<sub>2</sub>. *Mar. Biol.* **80**: 247–253. doi:10.1007/bf00392819
- Schneider, B., K. Eilola, K. Lukkari, B. Müller-Karulis, and T. Neumann. 2015. Environmental impacts—Marine biogeochemistry, p. 337–361. In BACC II Author Team [ed.], Second assessment of climate change for the Baltic Sea basin. Berlin: Springer.
- Schneider, B., and J. D. Müller. 2018. Biogeochemical transformations in the Baltic Sea. Springer Oceanography: Springer International Publishing.
- Sjötun, K. 1993. Seasonal lamina growth in two age groups of *Laminaria saccharina* (L.) Lamour in Western Norway. *Bot. Mar.* **36**: 433–441. doi:10.1515/botm.1993.36.5.433
- Sjötun, K., and K. Gunnarsson. 1995. Seasonal growth pattern of an Icelandic *Laminaria* population (section Simplicies, Laminariaceae, Phaeophyta) containing solid- and hollow-stiped plants. *Eur. J. Phycol.* **30**: 281–287. doi:10.1080/09670269500651061
- Smith, R. C., and K. S. Baker. 1978. Optical classification of natural waters. *Limnol. Oceanogr.* **23**: 260–267.
- Solidoro, C., G. Pecelik, R. Pastres, D. Franco, and C. Dejak. 1997. Modelling macroalgae (*Ulva rigida*) in the Venice lagoon: Model structure identification and first parameters estimation. *Ecol. Model.* **94**: 191–206. doi:10.1016/S0304-3800(96)00025-7
- Steele, J. H. 1962. Environmental control of photosynthesis in the sea. *Limnol. Oceanogr.* **7**: 137–150. doi:10.4319/lo.1962.7.2.0137
- Sunday, J. M., A. E. Bates, and N. K. Dulvy. 2012. Thermal tolerance and the global redistribution of animals. *Nat. Clim. Chang.* **2**: 686–690. doi:10.1038/nclimate1539
- Takolander, A., M. Cabeza, and E. Leskinen. 2017. Climate change can cause complex responses in Baltic Sea macroalgae: A systematic review. *J. Sea Res.* **123**: 16–29. doi:10.1016/j.seares.2017.03.007
- Torn, K., D. Krause-Jensen, and G. Martin. 2006. Present and past depth distribution of bladderwrack (*Fucus vesiculosus*) in the Baltic Sea. *Aquat. Bot.* **84**: 53–62. doi:10.1016/j.aquabot.2005.07.011
- Trancoso, A. R., S. Saraiva, L. Fernandes, P. Pina, P. Leitão, and R. Neves. 2005. Modelling macroalgae using a 3D hydrodynamic-ecological model in a shallow, temperate estuary. *Ecol. Model.* **187**: 232–246. doi:10.1016/j.ecolmodel.2005.01.054
- van der Molen, J., P. Ruardij, K. Mooney, and others. 2017. Modelling potential production and environmental effects of macroalgae farms in UK and Dutch coastal waters. *Biogeosciences* **15**: 1123–1147. doi:10.5194/bg-15-1123-2018
- van't Hoff, J. H. 1884. Études de dynamique chimique. Amsterdam: F. Muller.
- Wahl, M., and M. E. Hay. 1995. Associational resistance and shared doom: effects of epibiosis on herbivory. *Oecologia* **102**: 329–340. doi:10.1007/BF00329800
- Wahl, M., and others. 2010. Ecology of antifouling resistance in the bladder wrack *Fucus vesiculosus*: patterns of micro-fouling and antimicrobial protection. *Mar. Ecol. Prog. Ser.* **411**: 33–48. doi:10.3354/meps08644
- Wahl, M., and others. 2011. Stress ecology in *Fucus*: Abiotic, biotic and genetic interactions. *Adv. Mar. Biol.* **59**: 37–105. doi:10.1016/B978-0-12-385536-7.00002-9
- Wahl, M., and others. 2015a. The responses of brown macroalgae to environmental change from local to global scales: direct versus ecologically mediated effects. *Perspect. Phycol.* **2**: 11–30. doi:10.1127/pip/2015/0019
- Wahl, M., and others. 2015b. A mesocosm concept for the simulation of near-natural shallow underwater climates: The Kiel Outdoor Benthocosms (KOB). *Limnol. Oceanogr. Methods* **13**: 651–663. doi:10.1002/lom3.10055
- Wahl, M., F. J. Werner, B. Buchholz, and others. 2019. Season affects strength and direction of the interactive impacts of ocean warming and biotic stress in a coastal seaweed ecosystem. *Limnol. Oceanogr.* 1–21. doi:10.1002/lno.11350
- Wallentinus, I. 1984. Comparisons of nutrient uptake rates for Baltic macroalgae with different thallus morphologies. *Mar. Biol.* **80**: 215–225. doi:10.1007/BF02180189

- Wanninkhof, R., W. E. Asher, D. T. Ho, C. Sweeney, and W. R. McGillis. 2009. Advances in quantifying air-sea gas exchange and environmental forcing. *Ann. Rev. Mar. Sci.* **1**: 213–244. doi:[10.1146/annurev.marine.010908.163742](https://doi.org/10.1146/annurev.marine.010908.163742)
- Watson, D. J. 1947. Comparative physiological studies on the growth of field crops. *Ann. Bot.* **11**: 41–76. doi:[10.1093/oxfordjournals.aob.a083148](https://doi.org/10.1093/oxfordjournals.aob.a083148)
- Weiss, R. F. 1974. Carbon dioxide in water and seawater: the solubility of a non-ideal gas. *Mar. Chem.* **2**: 203–215. doi:[10.1016/0304-4203\(74\)90015-2](https://doi.org/10.1016/0304-4203(74)90015-2)
- Werner, F. J., A. Graiff, and B. Matthiessen. 2016. Temperature effects on seaweed-sustaining top-down control vary with season. *Oecologia* **180**: 889–901. doi:[10.1007/s00442-015-3489-x](https://doi.org/10.1007/s00442-015-3489-x)
- Wikström, S. A., and L. Kautsky. 2007. Structure and diversity of invertebrate communities in the presence and absence of canopy-forming *Fucus vesiculosus* in the Baltic Sea. *Estuar. Coast. Shelf Sci.* **72**: 168–176. doi:[10.1016/j.ecss.2006.10.009](https://doi.org/10.1016/j.ecss.2006.10.009)
- Zaldívar, J. M., F. S. Bacelar, S. Dueri, D. Marinov, P. Viaroli, and E. Hernández-García. 2009. Modeling approach to regime shifts of primary production in shallow coastal ecosystems. *Ecol. Model.* **220**: 3100–3110. doi:[10.1016/j.ecolmodel.2009.01.022](https://doi.org/10.1016/j.ecolmodel.2009.01.022)

### Conflict of interest

The authors declare that the research was conducted in the absence of any commercial or financial, as well as non-financial relationships that could be construed as a potential conflict of interest.

### Acknowledgments

We gratefully thank all members of the BIOACID Phase III Theme “Shifts in benthic ecosystems and their services” for their cooperation and support. We thank Janet Reid for linguistic revision and two reviewers for valuable comments. This research was funded by the Project BIOACID Phase III of the German Federal Ministry of Education and Research (BMBF; FKZ 03F0728K) and the DFG project (GR5088/2-1).

Submitted 12 December 2018

Revised 30 September 2019

Accepted 30 January 2020

Associate editor: George Waldbusser